Electronic Supplementary Material (ESI) for Physical Chemistry Chemical Physics.

Supporting Information

The unified quantum mechanical structure of tubular molecular rotors with multiple equivalent global minimum structures: The 18*C_{2h} → D_{9d} case of La-[B_2@B_{18}]-La

Xiao-Qin Lu,[a,b] Yuan Man,[a,c] Vincent Rußl,[d] Yonghong Xu,[a] Yonggang Yang*[a,c] and Si-Dian Li*[b]

[a] *State Key Laboratory of Quantum Optics and Quantum Optics Devices, Institute of Laser Spectroscopy, Shanxi University, Taiyuan 0300006, P. R. China.*
[b] *Nanocluster Laboratory, Institute of Molecular Science, Shanxi University, Taiyuan 030006, P. R. China.*
[c] *Collaborative Innovation Center of Extreme Optics, Shanxi University, Taiyuan 030006, P. R. China.*
[d] *Institut für Chemie und Biochemie, Freie Universität Berlin, 14195 Berlin, Germany.*

**E-mail: yggyang@sxu.edu.cn*; *lisidian@sxu.edu.cn*.

SI – Preamble

The following chapters SI I, SI II etc. are written in somewhat didactic style, for readers who are not familiar with e. g. the phenomenon of pseudo-rotations, permutations of equivalent nuclei, the role of nuclear spin isomers, or applications of cyclic molecular symmetry groups to quantum mechanically unified structures of the oriented tubular rotors. These chapters refer to Figures 1,2,3 of the main text and to Figures S1, S2 etc. and to Tables S1, S2 etc. which are compiled at the beginning of SI.

Table of Contents

Figure S3: a Vibrational frequencies and irreducible representations (IRREPs) of the vibrational normal modes of eighteen equivalent global minimum structures (GMs) and transition states (TSs) of La-[B_2@B_{18}]-La. **b** Vector arrow plots of two selected normal modes of three GMs and TSs. They are directed approximately along the rotational/pseudo-rotational paths of all nuclei. **c** Superposition of all vector arrow plots of the two selected normal modes of all GMs and all TSs.

Figure S4: Five perspective views of (**a**) the superposition of 18 GMs and 18 TSs and (**b**) the unified quantum mechanical structure with 18 interacting GMs of the oriented La-[B_2@B_{18}]-La.

Figure S5: Eigenenergies and eigenfunctions of selected rotational/pseudo-rotational eigenstates of the oriented tubular molecular rotor La-[B_2@B_{18}]-La.

Figure S6: The cyclic sequences of the reference coordinates of the nucleus of the bearing at the reference angle $\Phi_1 = 10\,°$, *versus* the azimuthal angle of the molecular wheel of the oriented model La-[B_2@B_{18}]-La, together with the pseudo-rotational paths which pass through these sequences.

Figure S7: a Cyclic sequence of the Cartesian coordinates X_j, Y_j of the nucleus of the bearing at the reference angle $\Phi_1 = 10\,°$, with parametric dependence on the azimuthal angle of the molecular wheel of the oriented La-[B_2@B_{18}]-La, and with the pseudo-rotational path which passes through this sequence. **b** Vector arrows attached to the balls shown in panel a, as explained for Figure S3c. The vectors at the TSs correlate well with the motions along the pseudo-rotational path.

Table S1: Permutations of the boron nuclei of the tubular bearing and of the molecular wheel of the reference global minimum structure GM_1 for the generation of the other GM_2, …, GM_{18} of the tubular rotor La-[B_2@B_{18}]-La.

Table S2: **a** Coordinates of the boron nuclei of the tubular bearing of the reference global minimum structure GM_1 and the transition state $TS_{18,1}$ of the oriented rotor La-[B_2@B_{18}]-La. **b** Coordinates of all (=18) boron nuclei of the tubular bearing of all (=18) global minimum structures and transitions states of the oriented rotor La-[B_2@B_{18}]-La.

Table S3: Rotational/pseudo-rotational energies and irreducible representations of the cyclic molecular symmetry group C_{18}(M) of the 54 lowest eigenstates of the oriented tubular rotor La-[B_2@B_{18}]-La.

SI I: The generation of all global minimum structures of the oriented tubular rotor La-[B_2@B_{18}]-La

SI II: The generation of all transition states of the oriented tubular rotor La-[B_2@B_{18}]-La

SI III: The cyclic molecular symmetry group C_{18}(M) of the oriented tubular rotor La-[B_2@B_{18}]-La

SI IV: Solution of the Schrödinger equation for the model of the rotating molecular wheel in the pseudo-rotating bearing of the oriented tubular rotor La-[B_2@B_{18}]-La

SI V: The effective moment of inertia of the rotation of the molecular wheel in the pseudo-rotating tubular bearing of the oriented rotor La-[B_2@B_{18}]-La

SI VI: The nuclear coordinates of 18 equivalent global minimum structures and 18 transition states of the oriented tubular rotor La-[B_2@B_{18}]-La

SI VII: The rotating molecular wheel in the pseudo-rotating tubular bearing of the oriented rotor La-[B_2@B_{18}]-La

SI VIII: Rotational and pseudo-rotational paths of the nuclei of the oriented tubular rotor La-[B_2@B_{18}]-La

SI IX: Support of the model of the rotating molecular wheel in the pseudo-rotating tubular bearing by vector arrow plots of two selected normal modes of La-[B_2@B_{18}]-La

Figure S1: Rainbow-colour-coded perspective views of eighteen equivalent global minimum structures GM_1, GM_2, …, GM_{18} of the oriented model tubular molecular rotor La-[B_2@B_{18}]-La. Nuclei in front and in the back are illustrated by large and small balls, respectively. The z-axis with the two La nuclei (grey balls, the one in front hides the one in the back) points to the viewer. Results calculated at the PBE0 level of quantum chemistry, cf. SI VI-A.

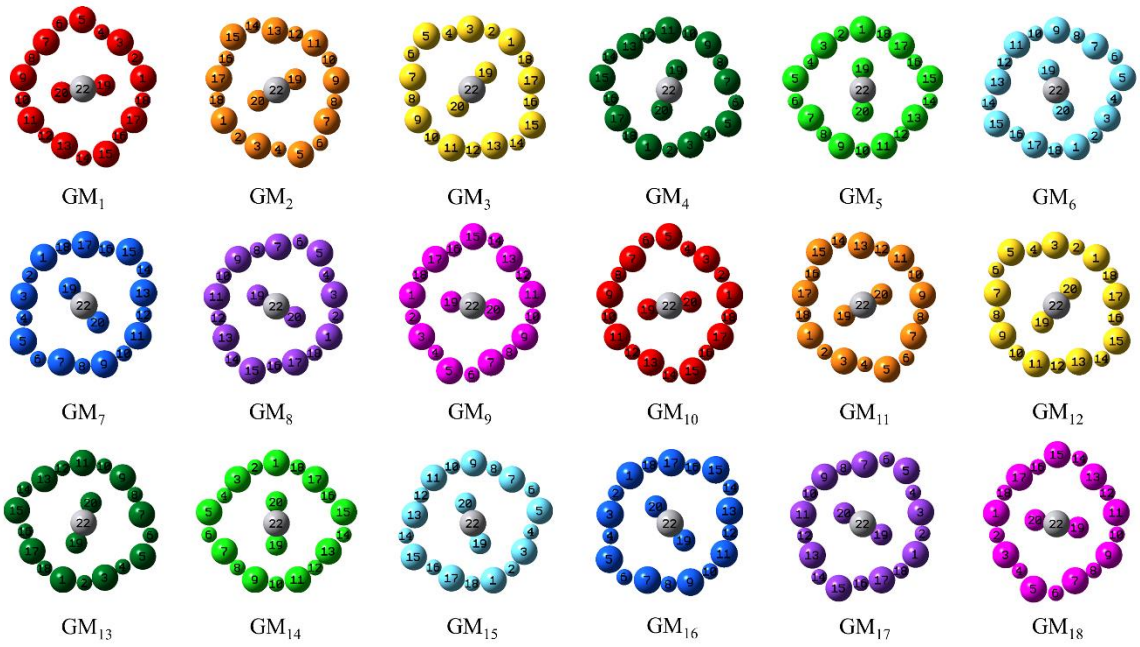

Figure S2: Rainbow-colour-coded perspective views of eighteen equivalent transition states $TS_{18,1}$, $TS_{1,2}$, …, $TS_{17,18}$ of the oriented model tubular molecular rotor La-[B_2@B_{18}]-La. The notations are as in Figure S1. Results calculated at the PBE0 level of quantum chemistry, cf. SI VI-A.

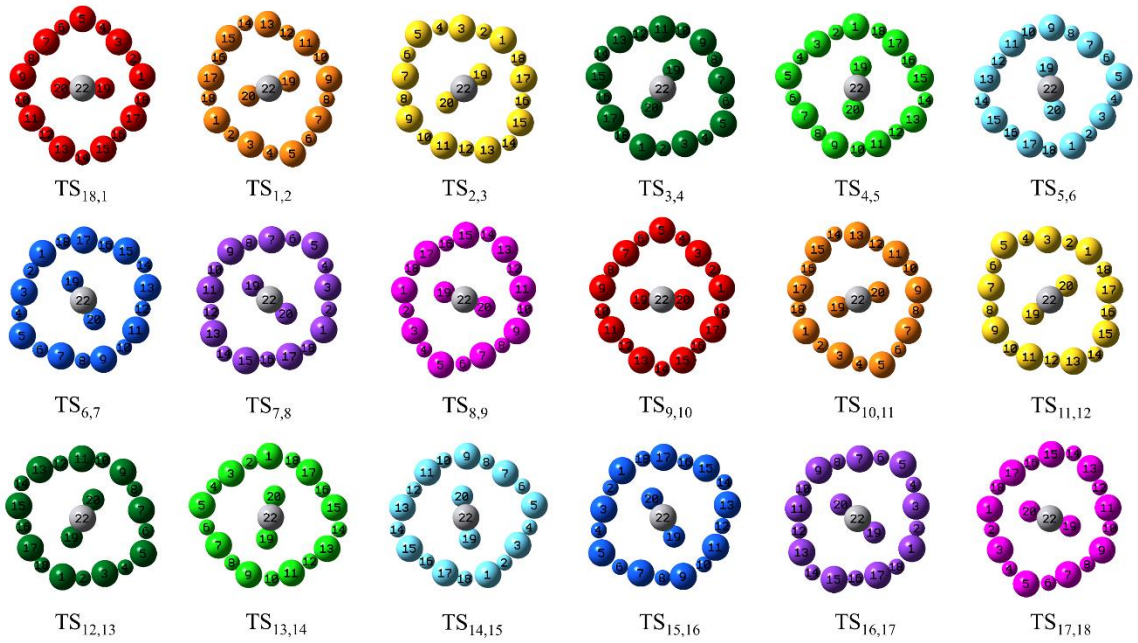

Figure S3: a Vibrational frequencies and irreducible representations (IRREPs) of the vibrational normal modes of eighteen equivalent global minimum structures (GM, cf. Figure S1) and transition states (TS, cf. Figure S2) of La-[B_2@B_{18}]-La. The molecular point group is C_{2h} for GM, and also for TS. The horizontal arrows point to the second lowest b_g mode (234.79 c cm^{-1}) of GM and to the b_g mode with imaginary frequency (217.84i c cm^{-1}) of TS. **b** Perspective views in opposite z-direction of the rainbow-colour-coded vector arrow plots of the two selected b_g modes of three GMs (filled circles) and TSs (open circles). Large circles are in front (Z > 0), small circles are in the back (Z < 0). The arrows are directed approximately along the rotational/pseudo-rotational paths of the nuclei. **c** Superposition of all (18+18) rainbow-colour-coded vector arrow plots of the two selected b_g modes of all GMs and TSs. Results calculated at the PBE0 level of quantum chemistry, cf. SI VI-A.

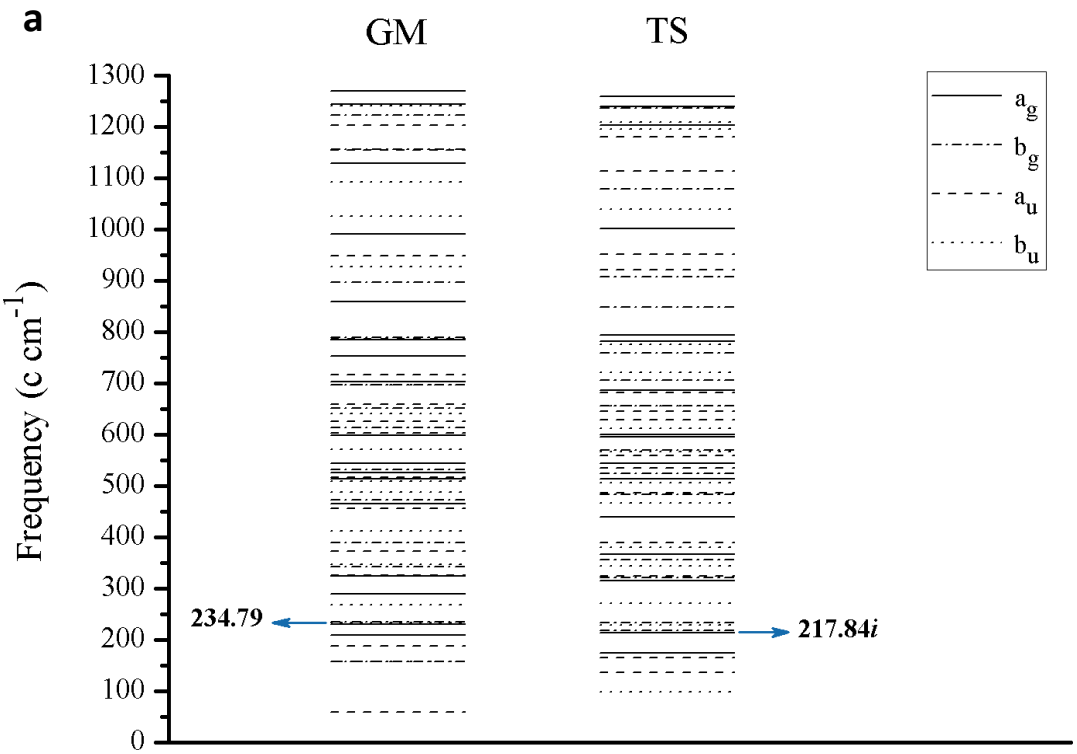

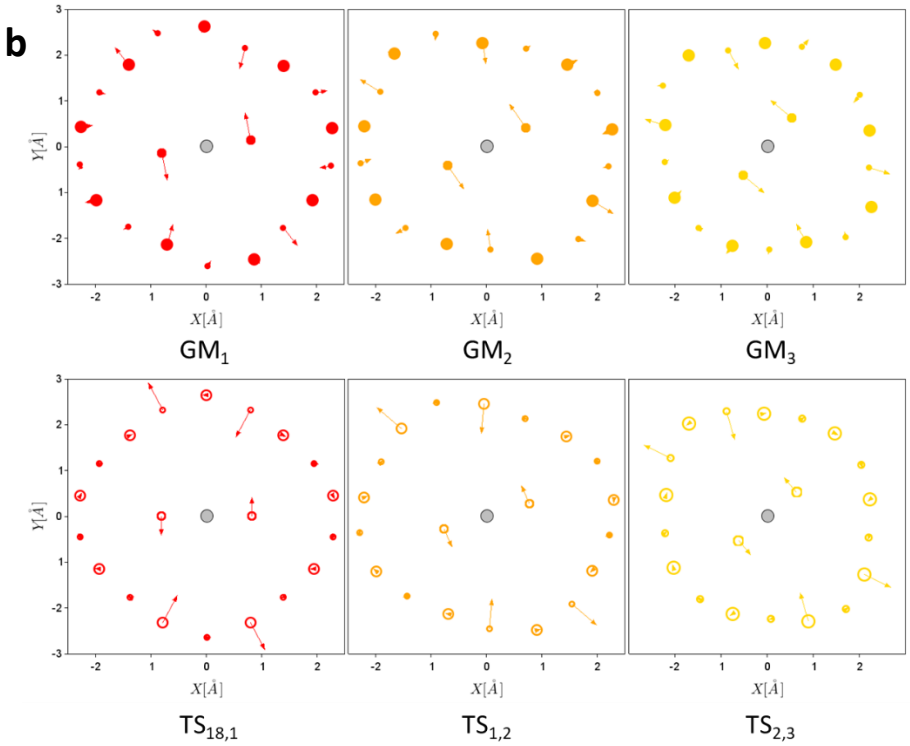
b
Y[Å]
X[Å]
GM1
GM2
GM3
TS18,1
TS1,2
TS2,3

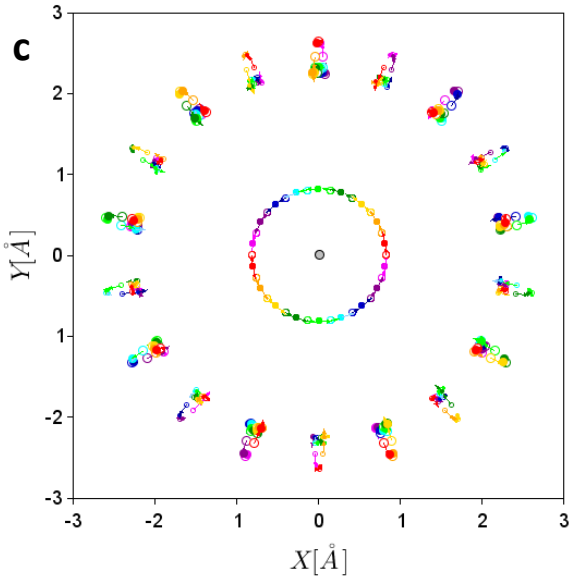
c
Y[Å]
X[Å]

Figure S4: Five perspective views of (**a**) the superposition of 18 rainbow-color-coded global minimum structures (GMs, full balls) and transitions states (TSs, open balls) and (**b**) the unified quantum mechanical structure with 18 interacting GMs of the oriented La-[B_2@B_{18}]-La. The zig-zag-lines guide the eye along the staggered sequence of the eighteen nuclei of the tubular bearing of the rotor. The 18 loops illustrate the pseudo-rotational paths of the 18 nuclei of the bearing. The insert shows a magnification of one of these pseudo-rotational paths. The two metal nuclei on the z-axis are illustrated by grey balls. In (**a**), the straight dashed lines from the metal nuclei to the two boron nuclei of the molecular wheel of the rotor illustrate 18 La-B_2-La rhombi of the 18 GMs. The rotational paths of the two nuclei of the wheel are illustrated by circles. In (**b**), the dashed lines illustrate the 18-cornered double cone of the unified structure.

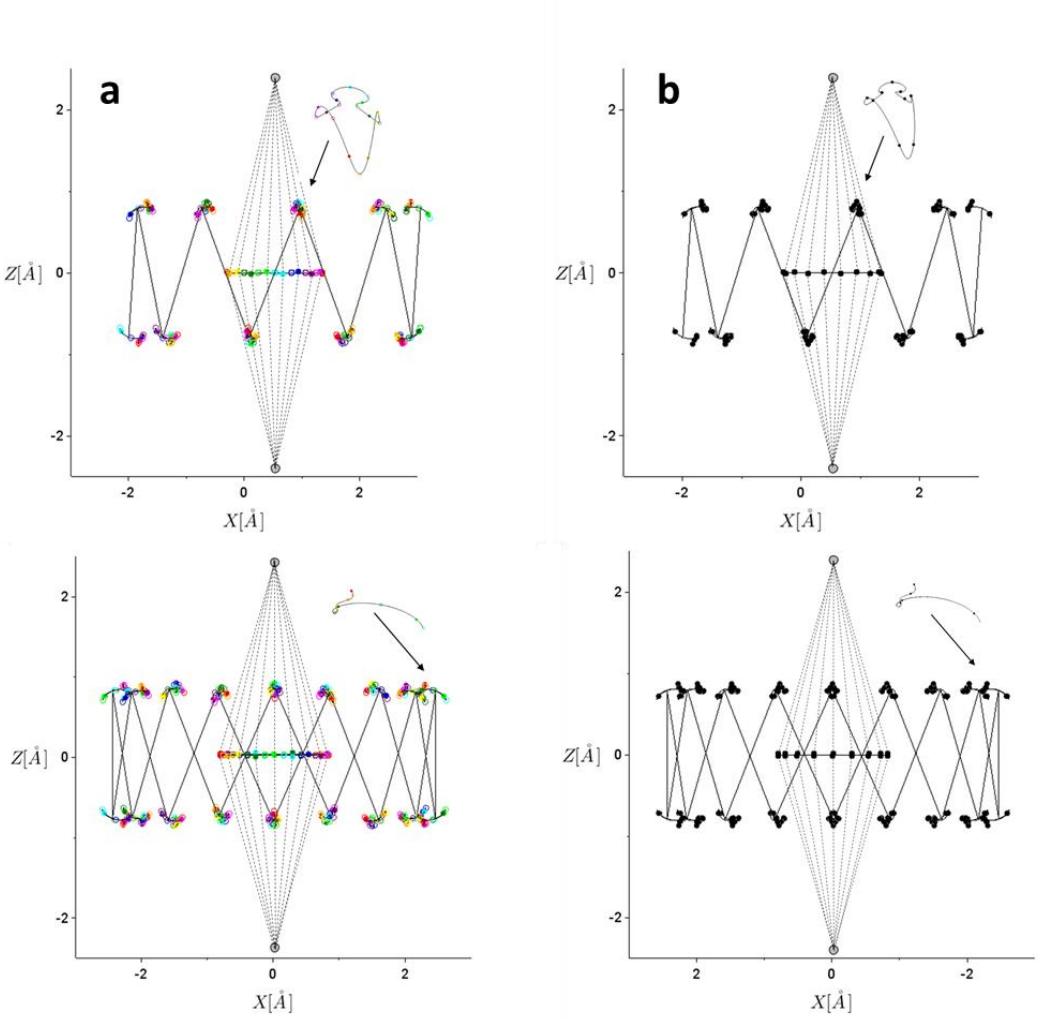

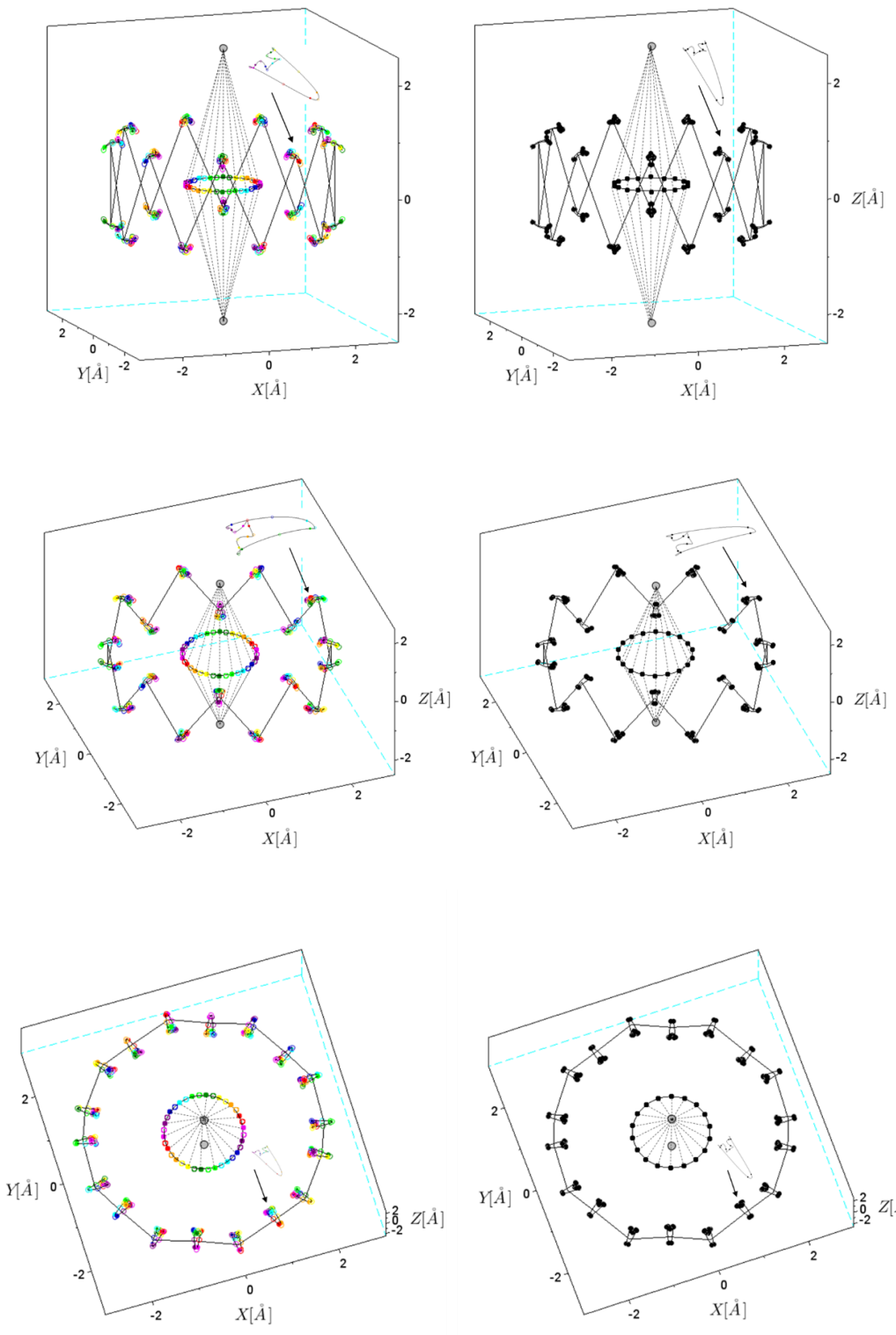
Y[Å]
X[Å]
Z[Å]

Figure S5: Eigenenergies E_m (m=0,17,18,35,36,53) and eigenfunctions Ψ_m (m=0,18,36,53) of selected rotational/pseudo-rotational eigenstates of the oriented tubular molecular rotor La-[B_2@B_{18}]-La. The levels serve as base lines for the eigenfunctions. They are embedded in the model potential V versus angle φ which specifies the rotation of the molecular wheel (B_2) in the pseudo-rotating tubular bearing (B_{18}), compare with Figure 3. All energies E_0 – E_{53} are below the potential barrier. The energy levels $E_{m=0}$ and $E_{m=17}$ as well as $E_{m=18}$ and $E_{m=35}$ appear superimposed, but this is a consequence of the low graphical resolution; their accurate values are non-degenerate, as listed in Table S3. The densities $\rho_m = |\Psi_m|^2$ look the same in each of the eighteen equivalent potential wells – this means that the eighteen equivalent global minimum structures (GMs) of La-[B_2@B_{18}]-La are populated with the same probability.

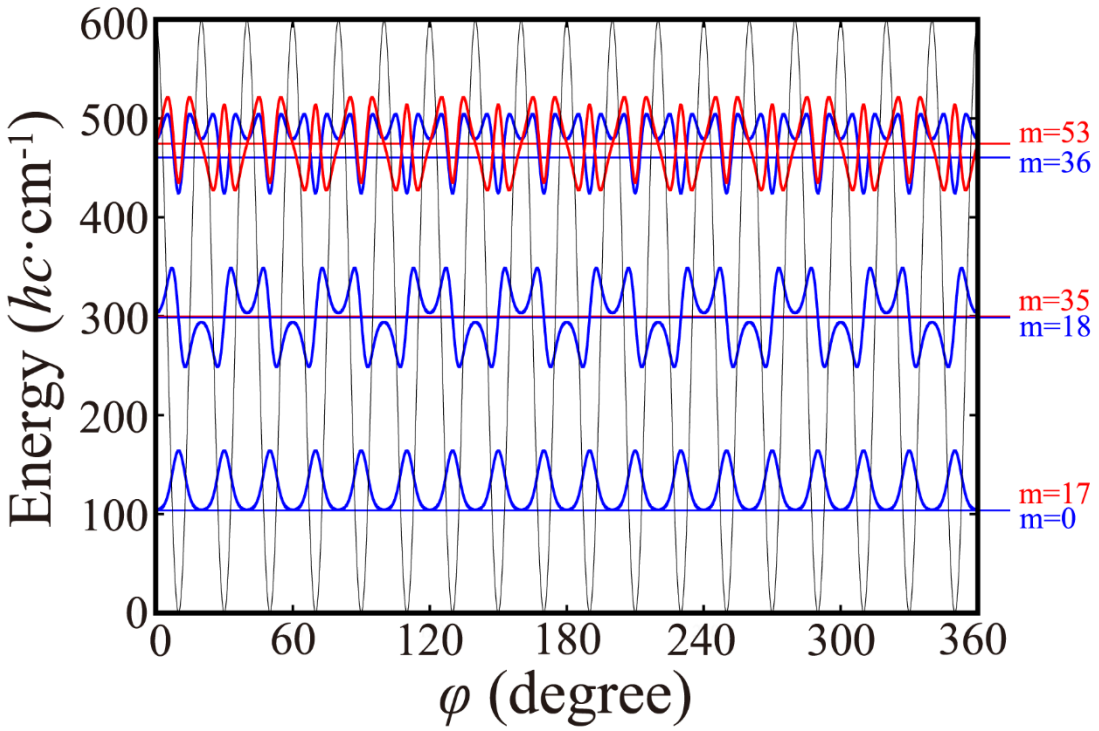

Figure S6: The cyclic sequences **a** of the cylindrical reference radial coordinate R_j, **b** the deviation angle $-\Delta\Phi_j$, and **c** the Cartesian coordinates X_j, Y_j, $|Z_j|$ of the nucleus of the bearing at the reference angle $\Phi_1 = 10$ °, *versus* the azimuthal angle of the molecular wheel of the model La-[B_2@B_{18}]-La back-rotated by $\Phi_1 = 10$ °, that means *versus* $\phi_j = \varphi_j - \Phi_1$, j=1, 2, …,36, 37≡1. Alternating filled and open circles refer to global minimum structures and transition states, respectively, from GM_1 (ϕ_1=0 °, j=1) *via* $TS_{1,2}$ (ϕ_2=10 °, j=2), GM_2 (ϕ_3=20 °, j=3), ... , GM_{18} (ϕ_{35}=340 °, j=34), $TS_{18,1}$ (ϕ_{36}=350 °, j=36 °) back to GM_1 ($\phi_1 = 360° \equiv 0°$, j = 37 ≡ 1), cf. Section SI VII. The pseudo-rotational paths which pass through these sequences are calculated by means of least square fits of symmetry-adapted Fourier series, cf. Section SI VIII.

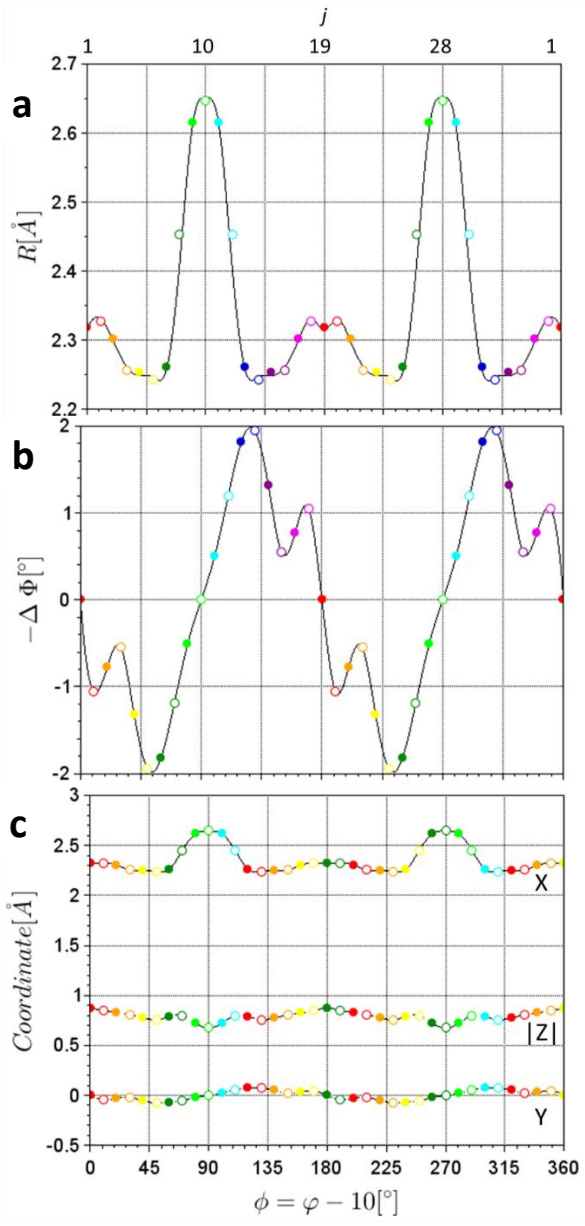

Figure S7: a Two-dimensional (2d) projection of the cyclic sequence of the Cartesian reference coordinates X_j, Y_j, $|Z_j|$ of the nucleus of the bearing at the reference angle $\Phi_1 = 10\,°$, with parametric dependence on the azimuthal angle of the molecular wheel of the model La-[B_2@B_{18}]-La back-rotated by Φ_1, that means depending on $\phi_j = \varphi_j - \Phi_1$, j = 1, 2, …,35, 36. Alternating filled and open circles indicate alternating global minimum structures (GMs) and transition states (TSs), as in Figure S4. The smooth pseudo-rotational paths which pass through these sequences are calculated by means of least square fits of symmetry-adapted Fourier series, cf. Chapter SI VIII. **b** Vector arrows attached to the balls shown in panel a. The vectors are generated from the selected b_g normal modes of the GMs and TSs, as explained for Figure S3c. The vectors at the TSs correlate well with the motions along the pseudo-rotational path.

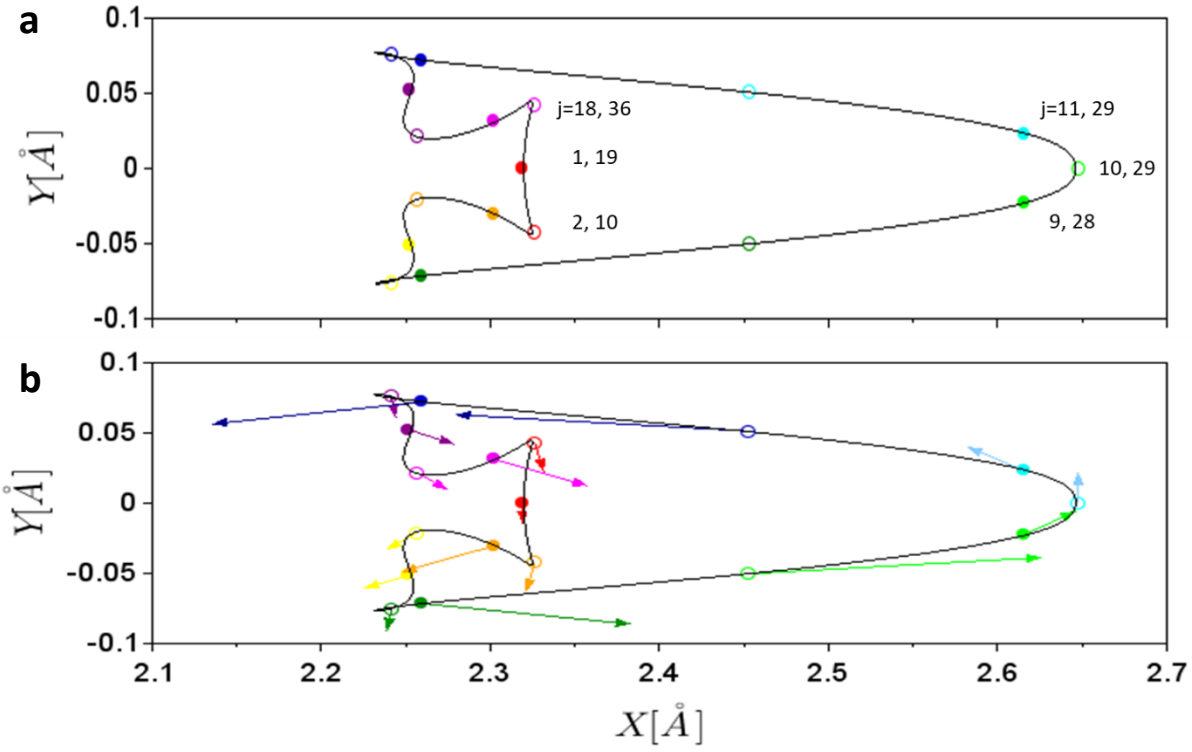

Table S1: Permutations of the cyclic molecular symmetry group C_{18}(M) for the boron nuclei of the tubular bearing (1-18) and of the molecular wheel (19, 20) of the reference global minimum structure GM_1 for the generation of the other GM_2, …, GM_{18} of the oriented molecular rotor La-[B_2@B_{18}]-La.*

P_k	g_p^k	permutation
P_1	g_p	(1 9 17 7 15 5 13 3 11) (2 10 18 8 16 6 14 4 12) (19 20)
P_2	g_p^2	(1 17 15 13 11 9 7 5 3) (2 18 16 14 12 10 8 6 4)
P_3	g_p^3	(1 7 13) (3 9 15) (5 11 17) (2 8 14) (4 10 16) (6 12 18) (19 20)
P_4	g_p^4	(1 15 11 7 3 17 13 9 5) (2 16 12 8 4 18 14 10 6)
P_5	g_p^5	(1 5 9 13 17 3 7 11 15) (2 6 10 14 18 4 8 12 16) (19 20)
P_6	g_p^6	(1 13 7) (3 15 9) (5 17 11) (2 14 8) (4 16 10) (6 18 12)
P_7	g_p^7	(1 3 5 7 9 11 13 15 17) (2 4 6 8 10 12 14 16 18) (19 20)
P_8	g_p^8	(1 11 3 13 5 15 7 17 9) (2 12 4 14 6 16 8 18 10)
P_9	g_p^9	(19 20)
P_{10}	g_p^{10}	(1 9 17 7 15 5 13 3 11) (2 10 18 8 16 6 14 4 12)
P_{11}	g_p^{11}	(1 17 15 13 11 9 7 5 3) (2 18 16 14 12 10 8 6 4) (19 20)
P_{12}	g_p^{12}	(1 7 13) (3 9 15) (5 11 17) (2 8 14) (4 10 16) (6 12 18)
P_{13}	g_p^{13}	(1 15 11 7 3 17 13 9 5) (2 16 12 8 4 18 14 10 6) (19 20)
P_{14}	g_p^{14}	(1 5 9 13 17 3 7 11 15) (2 6 10 14 18 4 8 12 16)
P_{15}	g_p^{15}	(1 13 7) (3 15 9) (5 17 11) (2 14 8) (4 16 10) (6 18 12) (19 20)
P_{16}	g_p^{16}	(1 3 5 7 9 11 13 15 17) (2 4 6 8 10 12 14 16 18)
P_{17}	g_p^{17}	(1 11 3 13 5 15 7 17 9) (2 12 4 14 6 16 8 18 10) (19 20)
P_{18}(=E)	g_p^{18}(=e)	(1)

- g_p denotes the generator of the permutations. E(e) denote the identity. For the details, see SI III.

Table S2: **a** Cylindrical coordinates of the boron nuclei of the tubular bearing of the reference global minimum structure GM_1 and the transition state $TS_{18,1}$ of the oriented rotor La-[B_2@B_{18}]-La.[a] **b** Coordinates of all (=18) boron nuclei of the tubular bearing of all (=18) global minimum structures and transitions states of the oriented rotor La-[B_2@B_{18}]-La.[b] Results calculated at the PBE0 level of quantum chemistry, cf. SI VI-A.

a

i	Φ_i[°]	j	φ_j[°]	$R_j=R_i^{TS}$, R_i^{GM} [Å]	$\Delta\Phi_j=\Delta\Phi_i^{TS}$, $\Delta\Phi_i^{GM}$ [°]	$Z_j=Z_i^{TS}$, Z_i^{GM} [Å]
1	10	0	0	2.3266	-1.0524	-0.8495
1	10	1	10	2.3187	0	0.8718
2	30	2	20	2.3266	1.0555	0.8497
2	30	3	30	2.3019	0.7724	-0.8245
3	50	4	40	2.2566	0.5481	-0.8029
3	50	5	50	2.2524	1.3204	0.7749
4	70	6	60	2.2425	1.9501	0.7557
4	70	7	70	2.2601	1.822	-0.7892
5	90	8	80	2.4530	1.1927	-0.7992
5	90	9	90	2.6155	0.5031	0.7202
6	110	10	100	2.6476	0.0012	0.6743
6	110	11	110	2.6155	-0.5031	-0.7202
7	130	12	120	2.4530	-1.1887	-0.7993
7	130	13	130	2.2601	-1.822	0.7892
8	150	14	140	2.2426	-1.9456	0.7557
8	150	15	150	2.2524	-1.3204	-0.7749
9	170	16	160	2.2565	-0.5429	-0.803
9	170	17	170	2.3019	-0.7724	0.8245
10	190	18	180	2.3266	-1.0524	0.8495
10	190	19	190	2.3187	0	-0.8718
11	210	20	200	2.3266	1.0555	-0.8497
11	210	21	210	2.3019	0.7724	0.8245
12	230	22	220	2.2566	0.5481	0.8029
12	230	23	230	2.2524	1.3204	-0.7749
13	250	24	240	2.2425	1.9501	-0.7557
13	250	25	250	2.2601	1.822	0.7892
14	270	26	260	2.4530	1.1927	0.7992
14	270	27	270	2.6155	0.5031	-0.7202
15	290	28	280	2.6476	0.0012	-0.6743
15	290	29	290	2.6155	-0.5031	0.7202
16	310	30	300	2.4530	-1.1887	0.7993
16	310	31	310	2.2601	-1.8220	-0.7892
17	330	32	320	2.2426	-1.9456	-0.7557
17	330	33	330	2.2524	-1.3204	0.7749
18	360	34	340	2.2565	-0.5429	0.803
18	360	35	350	2.3019	-0.7724	-0.8245
1	10	36	360	2.3266	-1.0524	-0.8495

b

TS / GM	k	$\varphi_{k,k+1}$[°]	i=1	2	3	4	5	6
		φ_k[°]	Φ_i[°]=10	30	50	70	90	110
$TS_{18,1}$	18	0	$1@T_{1,1}$	$2@T_{2,2}$	$3@T_{3,3}$	$4@T_{4,4}$	$5@T_{5,5}$	$6@T_{6,6}$
GM_1	1	10	$1@G_{1,1}$	$2@G_{2,2}$	$3@G_{3,3}$	$4@G_{4,4}$	$5@G_{5,5}$	$6@G_{6,6}$
$TS_{1,2}$	1	20	$9@T_{18,1}$	$10@T_{1,2}$	$11@T_{2,3}$	$12@T_{3,4}$	$13@T_{4,5}$	$14@T_{5,6}$
GM_2	2	30	$9@G_{18,1}$	$10@G_{1,2}$	$11@G_{2,3}$	$12@G_{3,4}$	$13@G_{4,5}$	$14@G_{5,6}$
$TS_{2,3}$	2	40	$17@T_{17,1}$	$18@T_{18,2}$	$1@T_{1,3}$	$2@T_{2,4}$	$3@T_{3,5}$	$4@T_{4,6}$
GM_3	3	50	$17@G_{17,1}$	$18@G_{18,2}$	$1@G_{1,3}$	$2@G_{2,4}$	$3@G_{3,5}$	$4@G_{4,6}$
$TS_{3,4}$	3	60	$7@T_{16,1}$	$8@T_{17,2}$	$9@T_{18,3}$	$10@T1_{,4}$	$11@T_{2,5}$	$12@T_{3,6}$
GM_4	4	70	$7@G_{16,1}$	$8@G_{17,2}$	$9@G_{18,3}$	$10@G_{1,4}$	$11@G_{2,5}$	$12@G_{3,6}$
$TS_{4,5}$	4	80	$15@T_{15,1}$	$16@T_{16,2}$	$17@T_{17,3}$	$18@T_{18,4}$	$1@T_{1,5}$	$2@T_{2,6}$
GM_5	5	90	$15@G_{15,1}$	$16@G_{16,2}$	$17@G_{17,3}$	$18@G_{18,4}$	$1@G_{1,5}$	$2@G_{2,6}$
$TS_{5,6}$	5	100	$5@T_{14,1}$	$6@T_{15,2}$	$7@T_{16,3}$	$8@T_{17,4}$	$9@T_{18,5}$	$10@T_{1,6}$
GM_6	6	110	$5@G_{14,1}$	$6@G_{15,2}$	$7@G_{16,3}$	$8@G_{17,4}$	$9@G_{18,5}$	$10@G_{1,6}$
$TS_{6,7}$	6	120	$13@T_{13,1}$	$14@T_{14,2}$	$15@T_{15,3}$	$16@T_{16,4}$	$17@T_{17,5}$	$18@T_{18,6}$
GM_7	7	130	$13@G_{13,1}$	$14@G_{14,2}$	$15@G_{15,3}$	$16@G_{16,4}$	$17@G_{17,5}$	$18@G_{18,6}$
$TS_{7,8}$	7	140	$3@T_{12,1}$	$4@T_{13,2}$	$5@T_{14,3}$	$6@T_{15,4}$	$7@T_{16,5}$	$8@T_{17,6}$
GM_8	8	150	$3@G_{12,1}$	$4@G_{13,2}$	$5@G_{14,3}$	$6@G_{15,4}$	$7@G_{16,5}$	$8@G_{17,6}$
$TS_{8,9}$	8	160	$11@T_{11,1}$	$12@T_{12,2}$	$13@T_{13,3}$	$14@T_{14,4}$	$15@T_{15,5}$	$16@T_{16,6}$
GM_9	9	170	$11@G_{11,1}$	$12@G_{12,2}$	$13@G_{13,3}$	$14@G_{14,4}$	$15@G_{15,5}$	$16@G_{16,6}$
$TS_{9,10}$	9	180	$1@T_{10,1}$	$2@T_{11,2}$	$3@T_{12,3}$	$4@T_{13,4}$	$5@T_{14,5}$	$6@T_{15,6}$
GM_{10}	10	190	$1@G_{10,1}$	$2@G_{11,2}$	$3@G_{12,3}$	$4@G_{13,4}$	$5@G_{14,5}$	$6@G_{15,6}$
$TS_{10,11}$	10	200	$9@T_{9,1}$	$10@T_{10,2}$	$11@T_{11,3}$	$12@T_{12,4}$	$13@T_{13,5}$	$14@T_{14,6}$
GM_{11}	11	210	$9@G_{9,1}$	$10@G_{10,2}$	$11@G_{11,3}$	$12@G_{12,4}$	$13@G_{13,5}$	$14@G_{14,6}$
$TS_{11,12}$	11	220	$17@T_{8,1}$	$18@T_{9,2}$	$1@T_{10,3}$	$2@T_{11,4}$	$3@T_{12,5}$	$4@T_{13,6}$
GM_{12}	12	230	$17@G_{8,1}$	$18@G_{9,2}$	$1@G_{10,3}$	$2@G_{11,4}$	$3@G_{12,5}$	$4@G_{13,6}$
$TS_{12,13}$	12	240	$7@T_{7,1}$	$8@T_{8,2}$	$9@T_{9,3}$	$10@T_{10,4}$	$11@T_{11,5}$	$12@T_{12,6}$
GM_{13}	13	250	$7@G_{7,1}$	$8@G_{8,2}$	$9@G_{9,3}$	$10@G_{10,4}$	$11@G_{11,5}$	$12@G_{12,6}$
$TS_{13,14}$	13	260	$15@T_{6,1}$	$16@T_{7,2}$	$17@T_{8,3}$	$18@T_{9,4}$	$1@T_{10,5}$	$2@T_{11,6}$
GM_{14}	14	270	$15@G_{6,1}$	$16@G_{7,2}$	$17@G_{8,3}$	$18@G_{9,4}$	$1@G_{10,5}$	$2@G_{11,6}$
$TS_{14,15}$	14	280	$5@T_{5,1}$	$6@T_{6,2}$	$7@T_{7,3}$	$8@T_{8,4}$	$9@T_{9,5}$	$10@T_{10,6}$
GM_{15}	15	290	$5@G_{5,1}$	$6@G_{6,2}$	$7@G_{7,3}$	$8@G_{8,4}$	$9@G_{9,5}$	$10@G_{10,6}$
$TS_{15,16}$	15	300	$13@T_{4,1}$	$14@T_{5,2}$	$15@T_{6,3}$	$16@T_{7,4}$	$17@T_{8,5}$	$18@T_{9,6}$
GM_{16}	16	310	$13@G_{4,1}$	$14@G_{5,2}$	$15@G_{6,3}$	$16@G_{7,4}$	$17@G_{8,5}$	$18@G_{9,6}$
$TS_{16,17}$	16	320	$3@T_{3,1}$	$4@T_{4,2}$	$5@T_{5,3}$	$6@T_{6,4}$	$7@T_{7,5}$	$8@T_{8,6}$
GM_{17}	17	330	$3@G_{3,1}$	$4@G_{4,2}$	$5@G_{5,3}$	$6@G_{6,4}$	$7@G_{7,5}$	$8@G_{8,6}$
$TS_{17,18}$	17	340	$11@T_{2,1}$	$12@T_{3,2}$	$13@T_{4,3}$	$14@T_{5,4}$	$15@T_{6,5}$	$16@T_{7,6}$
GM_{18}	18	350	$11@G_{2,1}$	$12@G_{3,2}$	$13@G_{4,3}$	$14@G_{5,4}$	$15@G_{6,5}$	$16@G_{7,6}$
$TS_{18,1}$	18	360	$1@T_{1,1}$	$2@T_{2,2}$	$3@T_{3,3}$	$4@T_{4,4}$	$5@T_{5,5}$	$6@T_{6,6}$

TS / GM	k	$\varphi_{k,k+1}$[°]	i=7	8	9	10	11	12
		φ_k[°]	Φ_i[°]=130	150	170	190	210	230
$TS_{18,1}$	18	0	$7@T_{7,7}$	$8@T_{8,8}$	$9@T_{9,9}$	$10@T_{10,10}$	$11@T_{11,11}$	$12@T_{12,12}$
GM_1	1	10	$7@G_{7,7}$	$8@G_{8,8}$	$9@G_{9,9}$	$10@G_{10,10}$	$11@G_{11,11}$	$12@G_{12,12}$
$TS_{1,2}$	1	20	$15@T_{6,7}$	$16@T_{7,8}$	$17@T_{8,9}$	$18@T_{9,10}$	$1@T_{10,11}$	$2@T_{11,12}$
GM_2	2	30	$15@G_{6,7}$	$16@G_{7,8}$	$17@G_{8,9}$	$18@G_{9,10}$	$1@G_{10,11}$	$2@G_{11,12}$
$TS_{2,3}$	2	40	$5@T_{5,7}$	$6@T_{6,8}$	$7@T_{7,9}$	$8@T_{8,10}$	$9@T_{9,11}$	$10@T_{10,12}$
GM_3	3	50	$5@G_{5,7}$	$6@G_{6,8}$	$7@G_{7,9}$	$8@G_{8,10}$	$9@G_{9,11}$	$10@G_{10,12}$
$TS_{3,4}$	3	60	$13@T_{4,7}$	$14@T_{5,8}$	$15@T_{6,9}$	$16@T_{7,10}$	$17@T_{8,11}$	$18@T_{9,12}$
GM_4	4	70	$13@G_{4,7}$	$14@G_{5,8}$	$15@G_{6,9}$	$16@G_{7,10}$	$17@G_{8,11}$	$18@G_{9,12}$
$TS_{4,5}$	4	80	$3@T_{3,7}$	$4@T_{4,8}$	$5@T_{5,9}$	$6@T_{6,10}$	$7@T_{7,11}$	$8@T_{8,12}$
GM_5	5	90	$3@GT_{3,7}$	$4@G_{4,8}$	$5@G_{5,9}$	$6@G_{6,10}$	$7@G_{7,11}$	$8@G_{8,12}$
$TS_{5,6}$	5	100	$11@T_{2,7}$	$12@T_{3,8}$	$13@T_{4,9}$	$14@T_{5,10}$	$15@T_{6,11}$	$16@T_{7,12}$
GM_6	6	110	$11@G_{2,7}$	$12@G_{3,8}$	$13@G_{4,9}$	$14@G_{5,10}$	$15@G_{6,11}$	$16@G_{7,12}$
$TS_{6,7}$	6	120	$1@T_{1,7}$	$2@T_{2,8}$	$3@T_{3,9}$	$4@T_{4,10}$	$5@T_{5,11}$	$6@T_{6,12}$
GM_7	7	130	$1@G_{1,7}$	$2@G_{2,8}$	$3@G_{3,9}$	$4@G_{4,10}$	$5@G_{5,11}$	$6@G_{6,12}$
$TS_{7,8}$	7	140	$9@T_{18,7}$	$10@T_{1,8}$	$11@T_{2,9}$	$12@T_{3,10}$	$13@T_{4,11}$	$14@T_{5,12}$
GM_8	8	150	$9@G_{18,7}$	$10@G_{1,8}$	$11@G_{2,9}$	$12@G_{3,10}$	$13@G_{4,11}$	$14@G_{5,12}$
$TS_{8,9}$	8	160	$17@T_{17,7}$	$18@T_{18,8}$	$1@T_{1,9}$	$2@T_{2,10}$	$3@T_{3,11}$	$4@T_{4,12}$
GM_9	9	170	$17@G_{17,7}$	$18@G_{18,8}$	$1@G_{1,9}$	$2@G_{2,10}$	$3@G_{3,11}$	$4@G_{4,12}$
$TS_{9,10}$	9	180	$7@T_{16,7}$	$8@T_{17,8}$	$9@T_{18,9}$	$10@T_{1,10}$	$11@T_{2,11}$	$12@T_{3,12}$
GM_{10}	10	190	$7@G_{16,7}$	$8@G_{17,8}$	$9@G_{18,9}$	$10@G_{1,10}$	$11@G_{2,11}$	$12@G_{3,12}$
$TS_{10,11}$	10	200	$15@T_{15,7}$	$16@T_{16,8}$	$17@T_{17,9}$	$18@T_{18,10}$	$1@T_{1,11}$	$2@T_{2,12}$
GM_{11}	11	210	$15@G_{15,7}$	$16@G_{16,8}$	$17@G_{17,9}$	$18@G_{18,10}$	$1@G_{1,11}$	$2@G_{2,12}$
$TS_{11,12}$	11	220	$5@T_{14,7}$	$6@T_{15,8}$	$7@T_{16,9}$	$8@T_{17,10}$	$9@T_{18,11}$	$10@T_{1,12}$
GM_{12}	12	230	$5@G_{14,7}$	$6@G_{15,8}$	$7@G_{16,9}$	$8@G_{17,10}$	$9@G_{18,11}$	$10@G_{1,12}$
$TS_{12,13}$	12	240	$13@T_{13,7}$	$14@T_{14,8}$	$15@T_{15,9}$	$16@T_{16,10}$	$17@T_{17,11}$	$18@T_{18,12}$
GM_{13}	13	250	$13@G_{13,7}$	$14@G_{14,8}$	$15@G_{15,9}$	$16@G_{16,10}$	$17@G_{17,11}$	$18@G_{18,12}$
$TS_{13,14}$	13	260	$3@T_{12,7}$	$4@T_{13,8}$	$5@T_{14,9}$	$6@T_{15,10}$	$7@T_{16,11}$	$8@T_{17,12}$
GM_{14}	14	270	$3@G_{12,7}$	$4@G_{13,8}$	$5@G_{14,9}$	$6@G_{15,10}$	$7@G_{16,11}$	$8@G_{17,12}$
$TS_{14,15}$	14	280	$11@T_{11,7}$	$12@T_{12,8}$	$13@T_{13,9}$	$14@T_{14,10}$	$15@T_{15,11}$	$16@T_{16,12}$
GM_{15}	15	290	$11@G_{11,7}$	$12@G_{12,8}$	$13@G_{13,9}$	$14@G_{14,10}$	$15@G_{15,11}$	$16@G_{16,12}$
$TS_{15,16}$	15	300	$1@T_{10,7}$	$2@T_{11,8}$	$3@T_{12,9}$	$4@T_{13,10}$	$5@T_{14,11}$	$6@T_{15,12}$
GM_{16}	16	310	$1@G_{10,7}$	$2@G_{11,8}$	$3@G_{12,9}$	$4@G_{13,10}$	$5@G_{14,11}$	$6@G_{15,12}$
$TS_{16,17}$	16	320	$9@T_{9,7}$	$10@T_{10,8}$	$11@T_{11,9}$	$12@T_{12,10}$	$13@T_{13,11}$	$14@T_{14,12}$
GM_{17}	17	330	$9@G_{9,7}$	$10@G_{10,8}$	$11@G_{11,9}$	$12@G_{12,10}$	$13@G_{13,11}$	$14@G_{14,12}$
$TS_{17,18}$	17	340	$17@T_{8,7}$	$18@T_{9,8}$	$1@T_{10,9}$	$2@T_{11,10}$	$3@T_{12,11}$	$4@T_{13,12}$
GM_{18}	18	350	$17@G_{8,7}$	$18@G_{9,8}$	$1@G_{10,9}$	$2@G_{11,10}$	$3@G_{12,11}$	$4@G_{13,12}$
$TS_{18,1}$	18	360	$7@T_{7,7}$	$8@T_{8,8}$	$9@T_{9,9}$	$10@T_{10,10}$	$11@T_{11,11}$	$12@T_{12,12}$

TS / GM	k	$\varphi_{k,k+1}$[°]	i=13	14	15	16	17	18
		φ_k[°]	Φ_i[°]=250	270	290	310	330	350
$TS_{18,1}$	18	0	$13@T_{13,13}$	$14@T_{14,14}$	$15@T_{15,15}$	$16@T_{16,16}$	$17@T_{17,17}$	$18@T_{18,18}$
GM_1	1	10	$13@G_{13,13}$	$14@G_{14,14}$	$15@G_{15,15}$	$16@G_{16,16}$	$17@G_{17,17}$	$18@G_{18,18}$
$TS_{1,2}$	1	20	$3@T_{12,13}$	$4@T_{13,14}$	$5@T_{14,15}$	$6@T_{15,16}$	$7@T_{16,17}$	$8@T_{17,18}$
GM_2	2	30	$3@G_{12,13}$	$4@G_{13,14}$	$5@G_{14,15}$	$6@G_{15,16}$	$7@G_{16,17}$	$8@G_{17,18}$
$TS_{2,3}$	2	40	$11@T_{11,13}$	$12@T_{12,14}$	$13@T_{13,15}$	$14@T_{14,16}$	$15@T_{15,17}$	$16@T_{16,18}$
GM_3	3	50	$11@G_{11,13}$	$12@G_{12,14}$	$13@G_{13,15}$	$14@G_{14,16}$	$15@G_{15,17}$	$16@G_{16,18}$
$TS_{3,4}$	3	60	$1@T_{10,13}$	$2@T_{11,14}$	$3@T_{12,15}$	$4@T_{13,16}$	$5@T_{14,17}$	$6@T_{15,18}$
GM_4	4	70	$1@G_{10,13}$	$2@G_{11,14}$	$3@G_{12,15}$	$4@G_{13,16}$	$5@G_{14,17}$	$6@G_{15,18}$
$TS_{4,5}$	4	80	$9@T_{9,13}$	$10@T_{10,14}$	$11@T_{11,15}$	$12@T_{12,16}$	$13@T_{13,17}$	$14@T_{14,18}$
GM_5	5	90	$9@G_{9,13}$	$10@G_{10,14}$	$11@G_{11,15}$	$12@G_{12,16}$	$13@G_{13,17}$	$14@G_{14,18}$
$TS_{5,6}$	5	100	$17@T_{8,13}$	$18@T_{9,14}$	$1@T_{10,15}$	$2@T_{11,16}$	$3@T_{12,17}$	$4@T_{13,18}$
GM_6	6	110	$17@G_{8,13}$	$18@G_{9,14}$	$1@G_{10,15}$	$2@G_{11,16}$	$3@G_{12,17}$	$4@G_{13,18}$
$TS_{6,7}$	6	120	$7@T_{7,13}$	$8@T_{8,14}$	$9@T_{9,15}$	$10@T_{10,16}$	$11@T_{11,17}$	$12@T_{12,18}$
GM_7	7	130	$7@G_{7,13}$	$8@G_{8,14}$	$9@G_{9,15}$	$10@G_{10,16}$	$11@G_{11,17}$	$12@G_{12,18}$
$TS_{7,8}$	7	140	$15@T_{6,13}$	$16@T_{7,14}$	$17@T_{8,15}$	$18@T_{9,16}$	$1@T_{10,17}$	$2@T_{11,18}$
GM_8	8	150	$15@G_{6,13}$	$16@G_{7,14}$	$17@G_{8,15}$	$18@G_{9,16}$	$1@G_{10,17}$	$2@G_{11,18}$
$TS_{8,9}$	8	160	$5@T_{5,13}$	$6@T_{6,14}$	$7@T_{7,15}$	$8@T_{8,16}$	$9@T_{9,17}$	$10qT_{10,18}$
GM_9	9	170	$5@G_{5,13}$	$6@G_{6,14}$	$7@G_{7,15}$	$8@G_{8,16}$	$9@G_{9,17}$	$10@G_{10,18}$
$TS_{9,10}$	9	180	$13@T_{4,13}$	$14@T_{5,14}$	$15@T_{6,15}$	$16@T_{7,16}$	$17@T_{8,17}$	$18@T_{9,18}$
GM_{10}	10	190	$13@G_{4,13}$	$14@G_{5,14}$	$15@G_{6,15}$	$16@G_{7,16}$	$17@G_{8,17}$	$18@G_{9,18}$
$TS_{10,11}$	10	200	$3@T_{3,13}$	$4@T_{4,14}$	$5@T_{5,15}$	$6@T_{6,16}$	$7@T_{7,17}$	$8@T_{8,18}$
GM_{11}	11	210	$3@G_{3,13}$	$4@G_{4,14}$	$5@G_{5,15}$	$6@G_{6,16}$	$7@G_{7,17}$	$8@G_{8,18}$
$TS_{11,12}$	11	220	$11@T_{2,13}$	$12@T_{3,14}$	$13@T_{4,15}$	$14@T_{5,16}$	$15@T_{6,17}$	$16@T_{7,18}$
GM_{12}	12	230	$11@G_{2,13}$	$12@G_{3,14}$	$13@G_{4,15}$	$14@G_{5,16}$	$15@G_{6,17}$	$16@G_{7,18}$
$TS_{12,13}$	12	240	$1@T_{1,13}$	$2@T_{2,14}$	$3@T_{3,15}$	$4@T_{4,16}$	$5@T_{5,17}$	$6@T_{6,18}$
GM_{13}	13	250	$1@G_{1,13}$	$2@G_{2,14}$	$3@G_{3,15}$	$4@G_{4,16}$	$5@G_{5,17}$	$6@G_{6,18}$
$TS_{13,14}$	13	260	$9@T_{18,13}$	$10@T_{1,14}$	$11@T_{2,15}$	$12@T_{3,16}$	$13@T_{4,17}$	$14@T_{5,18}$
GM_{14}	14	270	$9@G_{18,13}$	$10@G_{1,14}$	$11@G_{2,15}$	$12@G_{3,16}$	$13@G_{4,17}$	$14@G_{5,18}$
$TS_{14,15}$	14	280	$17@T_{17,13}$	$18@T_{18,14}$	$1@T_{1,15}$	$2@T_{2,16}$	$3@T_{3,17}$	$4@T_{4,18}$
GM_{15}	15	290	$17@G_{17,13}$	$18@G_{18,14}$	$1@G_{1,15}$	$2@G_{2,16}$	$3@G_{3,17}$	$4@G_{4,18}$
$TS_{15,16}$	15	300	$7@T_{16,13}$	$8@T_{17,14}$	$9@T_{18,15}$	$10@T_{1,16}$	$11@T_{2,17}$	$12@T_{3,18}$
GM_{16}	16	310	$7@G_{16,13}$	$8@G_{17,14}$	$9@G_{18,15}$	$10@G_{1,16}$	$11@G_{2,17}$	$12@G_{3,18}$
$TS_{16,17}$	16	320	$15@T_{15,13}$	$16@T_{16,14}$	$17@T_{17,15}$	$18@T_{18,16}$	$1@T_{1,17}$	$2@T_{2,18}$
GM_{17}	17	330	$15@G_{15,13}$	$16@G_{16,14}$	$17@G_{17,15}$	$18@G_{18,16}$	$1@G_{1,17}$	$2@G_{2,18}$
$TS_{17,18}$	17	340	$5@T_{14,13}$	$6@T_{15,14}$	$7@T_{16,15}$	$8@T_{17,16}$	$9@T_{18,17}$	$10@T_{1,18}$
GM_{18}	18	350	$5@G_{14,13}$	$6@G_{15,14}$	$7@G_{16,15}$	$8@G_{17,16}$	$9@G_{18,17}$	$10@G_{1,18}$
$TS_{18,1}$	18	360	$13@T_{13,13}$	$14@T_{14,14}$	$15@T_{15,15}$	$16@T_{16,16}$	$17@T_{17,17}$	$18@T_{18,18}$

Footnotes for Table S2:

[a] The reference angles for the nuclei of the oriented tubular bearing of La-[B_2@B_{18}]-La are at $\Phi_1 = 10°$, $\Phi_2 = 30°$, $\Phi_3 = 50°$, …, $\Phi_{18} = 350°$. In the reference global minimum structure GM_1, these are occupied by boron nuclei labeled i = 1, 2, 3, …, 18, respectively. The cylindrical coordinates of nucleus i in GM_1 at Φ_i are (R_i^{GM}, $\Phi_i + \Delta\Phi_i^{GM}$, Z_i^{GM}). The cylindrical coordinates of nucleus i in the reference transition state $TS_{18,1}$ at Φ_i are (R_i^{RS}, $\Phi_i + \Delta\Phi_i^{TS}$, Z_i^{TS}). For each label i, the entry for TS is on top of the entry for GM. The double sets of labels i can be mapped on labels j = 0, 1, 2, …, 36 with azimuthal angle φ_j, cf. Section SI VI.

[b] The short hand notation i_k@$G_{19-k+i,i}$ specifies the coordinates of the boron nucleus i_k of the tubular bearing of the global minimum structure GM_k of the oriented tubular rotor La-[B_2@B_{18}]-La at reference angle Φ_i, cf. eqn. (39) in SI VII and Table S2a. Likewise, the short hand notation i_k@$T_{18-k+i,i}$ specifies the coordinates of the boron nucleus i_k of the tubular bearing of the transition state $TS_{k,k+1}$ of the oriented tubular rotor La-[B_2@B_{18}]-La at reference angle Φ_i, cf. eqn. (42) in SI VII and Table S2a. The nucleus i of the references GM_1 or $TS_{18,1}$ at Φ_i is replaced by i_k in GM_k or $TS_{k,k+1}$ by the permutation P_{k-1} as listed in Table S1.

Table S3: Rotational/pseudo-rotational energies $E_m = E_{nl}$ and irreducible representations of the cyclic molecular symmetry group C_{18}(M) of the 54 lowest eigenstates of the oriented tubular rotor La-[B_2@B_{18}]-La[*]

Quantum number			Energy	Quantum number			Energy	Quantum number			Energy
m	l	n		m	l	n		m	l	n	
0	0	0	103.685	18	1	9	298.682	36	2	0	460.457
1,2	0	1,17	103.686	19,20	1	10,8	298.716	37,38	2	1,17	460.808
3,4	0	2,16	103.689	21,22	1	11,7	298.815	39,40	2	2,16	461.838
5,6	0	3,15	103.694	23,24	1	12,6	298.967	41,42	2	3,15	463.469
7,8	0	4,14	103.700	25,26	1	13,5	299.155	43,44	2	4,14	465.571
9,10	0	5,13	103.706	27,28	1	14,4	299.356	45,46	2	5,13	467.950
11,12	0	6,12	103.712	29,30	1	15,3	299.545	47,48	2	6,12	470.344
13,14	0	7,11	103.716	31,32	1	16,2	299.701	49,50	2	7,11	472.432
15,16	0	8,10	103.719	33,34	1	17,1	299.803	51,52	2	8,10	473.874
17	0	9	103.720	35	1	0	299.839	53	2	9	474.390

[*]All levels (in units of hc cm^{-1}) are below the potential barrier, V_b =599.27 hc cm^{-1}. The quantum numbers m=ln specify the energy bands l=0,1,2 and the irreducible representations Γ_n of the cyclic molecular symmetry group C_{18}(M).

SI I: The generation of all global minimum structures of the oriented tubular rotor La-[B_2@B_{18}]-La

Starting from the reference GM_1 of the oriented tubular molecular rotor La-[B_2@B_{18}]-La, one can generate the cyclic sequence GM_2, GM_3,…, GM_{18} of all global minimum structures by sequential applications of a "generator" g which comprises three operations, $g = \{g_r, g_a, g_p\}$ where g_r is a specific rotation of the molecular wheel in the bearing, g_a is the adjustment, or relaxation of the bearing to the new orientation of the rotated wheel, and g_p is a specific permutation of the labels of the boron nuclei. The first, second, …, seventeenth applications of g transform GM_1 into GM_2, then GM_2 into GM_3, …, GM_{17} into GM_{18}, respectively. If one adds another (= the eighteenth) application of g, then it transforms GM_{18} in a cyclic manner back to GM_1. One can also say that 1,2, …, 17, 18 applications of g, that means g, g^2, …, g^{17} and $e = g^{18}$ (the identity) transform GM_1 into GM_2, GM_3,…,GM_{18}, GM_1, symbolically

$$\begin{aligned} g &: GM_1 \rightarrow GM_2,\ GM_2 \rightarrow GM_3,\ \ldots,\ GM_{17} \rightarrow GM_{18},\ GM_{18} \rightarrow GM_1 \\ g^k &: GM_1 \rightarrow GM_{k+1} \text{ for } k=1,2,\ldots 17. \\ e = g^{18} &: GM_1 \rightarrow GM_1 \end{aligned} \quad (1)$$

The reference GM_1 and the resulting GM_2, …, GM_{18} are illustrated in Figure S1.

Let us now specify the operations of the generator $g = \{g_r, g_a, g_p\}$, starting with the rotation g_r of the wheel in the bearing of the tubular molecular rotor La-[B_2@B_{18}]-La. Since the goal is to generate eighteen equivalent GMs, g_r rotates the wheel by 360 ⁰/18 = 20 °, symbolically

$$\begin{aligned} g_r &: \varphi \rightarrow \varphi + 20° \bmod 360° \\ g_r^k &: \varphi \rightarrow \varphi + k*20° \bmod 360° \\ e_r = g_r^{18} &: \varphi \rightarrow \varphi \end{aligned} \quad (2)$$

The azimuthal angle of the reference GM_1 is set to $\varphi_1 = 10$ °. As consequence, the azimuthal angles φ_2, …, φ_{18} of the molecular wheel in GM_2, …., GM_{18} are equal to 30°, …, 350°.

The rotation of the wheel g_r in the bearing of the tubular molecular rotor La_2[B_2@B_{18}] is associated with the adjustment g_a of the bearing to the new position of the wheel, and with a specific permutation g_p of the labels of the boron nuclei. For didactic purposes, this will be explained by two examples. Let us first consider a rather simple case, namely application of g^2 on GM_1 in order to generate GM_3, cf. Figure 1. For reference, let us recall that GM_1 has C_{2h}

symmetry, and the two nuclei of the wheel labeled n = 19 and 20 and their nearest neighbors in the bearing – these are the nuclei 1 and 10 in the boron rings above and below the x-y-plane, respectively – are in the C_{2h} symmetry plane. Double application of g means that the wheel is rotated from φ_1 = 10 °by 2*20 °= 40 °to φ_3 = 50 °, eq. (2). If the rotation g_r^2 would be carried out in the rigid bearing without any nuclear relaxations and permutations, then the nuclei 19 and 20 would end up pointing towards the nuclei 3 and 12 of the bearing of GM_1, respectively, cf. Figure 1. The rotated nuclei 19, 20 and the non-rotated nuclei 3, 12, however, would no longer be in the symmetry plane – the C_{2h} symmetry of GM_1 would be broken. Clearly, the resulting overall shape of the rotor La-[B_2@B_{18}]-La would differ from GM_1 – it could no longer be a global minimum structure. To restore the global minimum structure, the bearing must adjust, or relax to the new position of the wheel. This adjustment g_a^2 has to restore in particular the C_{2h} symmetry with the nuclei 19, 20 of the wheel and two opposite nuclei of the bearing in the symmetry plane. This necessary condition requires that the adaption g_a^2 is equivalent to (but it is not the same as!) a hypothetical rotation of the bearing with respect to the wheel, by the same azimuthal angle as the wheel, i. e. by 40 °. This rotation would replace the original nuclear labels 3, 12 of GM_1 by 1, 10 in GM_3 so that the four nuclei 1,10,19,20 are back to the C_{2h} symmetry plane of GM_3. In fact, the combined rotations of the wheel and the bearing, both by the same angle 2*20 °, would correspond to the overall rotation of GM_1 by 2*20 °. The resulting GM_3 then looks like GM_1 rotated by 40 °, hence GM_3 is a global minimum structure like GM_1, cf. Figure 1.

After the discussion of the rotation g_r^2 of the wheel in the bearing and the adjustment g_a^2 of the bearing to the new position of the wheel, let us now address the associated permutation g_p^2 of the nuclear labels. For this purpose, we note that the order of the nuclei in the bearing is robust. As consequence, the replacement of the labels of the nuclei 3,12 in GM_1 by 1,10 in GM_3 implies the automatic replacement of all nuclear labels (1,2,3,4, …., 12, ...,17,18) in the tubular bearing of GM_1 by (17,18,1,2, …,10, …, 15,16) in GM_3, cf. Figure 1. Hence

$$g_p^2 = (1\ 17\ 15\ 13\ 11\ 9\ 7\ 5\ 3)\ (2\ 18\ 16\ 14\ 12\ 10\ 8\ 6\ 4). \qquad (3)$$

This cyclic notation of the permutation should be read as “the nuclear label 1 is replaced by 17, label 17 by 15,…, nuclear label 5 by 3, label 3 by 1 (*sic* !), nucleus 2 by 18,…, nucleus 12 by 10 (*sic* !),…, nucleus 4 by 2”. These replacements are verified by comparison of the nuclear labels in GM_1 and GM_3, see Figure 1. The cyclic notation in eqn. (3) shows that the odd-valued nuclear labels are permutated among each other, well separated from equivalent permutations of

the even-valued nuclear labels. This is a consequence of the robustness of the cyclic order of the boron nuclei in the two staggered, or interstitial rings of the tubular bearing – the exchange of any two boron nuclei with odd and even labels would imply the exchange of atoms in the rings above and below the x-y-plane, but this is unfeasible at low energies.

As second and slightly more demanding example, let us consider the application of g on GM_1, to generate GM_2 of the tubular molecular rotor La-[B_2@B_{18}]-La, cf. Figure 1. Here g_r rotates the molecular wheel in the bearing by 20 °. If this rotation would be carried out in an inert bearing without any permutations of the nuclear labels, the nuclei 19, 20 of the wheel would point towards the nuclei labeled 2 and 11 of the bearing of GM_1, cf. Figure 1. As for the first example, this structure would differ from the global minimum structure, and again, in order to restore it, the bearing has to adjust to the new position of the wheel. On first glance, the first example might suggest that this adjustment g_a should be equivalent to the rotation of the bearing by the same angle as the wheel, i.e. by 20 °. But this could not be successful because it would mean, for example, that the nucleus 2 in the reference GM_1 where it is below the x-y-plane should be replaced by nucleus 1 which is above the x-y-plane. This would call for nuclear motion from the boron ring of the tubular bearing below the x-y-plane to the other ring above the x-y-plane, but this is unfeasible in the oriented rotor La-[B_2@B_{18}]-La. The restoration of the global minimum structure GM_2 can be achieved, however, by an adjustment of the bearing which is equivalent to (but not the same as) a rotation of the bearing with respect to the wheel by 20 °+ 180 ° = 200 °. Figure 1 shows that now the nucleus 2 of the bearing in GM_1 is replaced by nucleus 10 in GM_2. This is feasible because both nuclei 2 and 10 are in the boron ring of the bearing below the x-y-plane. The replacement of nucleus 2 by 10 implies the automatic replacement of all labels (1,2,3, …,10,11, ….,17,18) of the nuclei of the tubular bearing in GM_1 by (9,10,11, ….,18,1, ……,8, 9) in GM_2, cf. Figure 1, due to the robustness of the cyclic order of the nuclei in the tubular bearing. Finally, the restoration of the shape of the bearing of GM_1 in GM_2 must also be accompanied by a small albeit absolutely necessary adjustment of the wheel, namely nucleus 19 should move from its position just below the x-y-plane to the corresponding position just above the x-y-plane, and *vice versa* for nucleus 20. This adjustment is equivalent to the exchange of nuclei 19 and 20. Summing up, GM_2 is generated from the reference GM_1 by

the generator $\mathbf{g = \{g_r, g_a, g_p\}}$ where

- g_r rotates the molecular wheel in the bearing,

$g_r : \varphi \rightarrow \varphi + 20°$

- g_a adjusts the shape of the bearing to the new azimuthal angle of the molecular wheel,

- g_p permutes the labels of the boron nuclei

$$g_p = (1\ 9\ 17\ 7\ 15\ 5\ 13\ 3\ 11)\ (2\ 10\ 18\ 8\ 16\ 6\ 14\ 4\ 12)\ (19\ 20) \qquad (4)$$

This permutation is mathematically equivalent to some number of permutations of pairs of nuclei with odd labels of the upper ring of the tubular bearing, plus the same number of permutations of pairs of nuclei with even labels of the lower ring, plus 1 for the permutation of the two nuclei of the wheel, hence it is equivalent to an odd number of permutations of pairs of boron nuclei. Since the boron nuclei are fermions, the total wavefunction of the tubular rotor must be anti-symmetric i. e. it must change sign upon each permutation of any pair of nuclei. Since g_p corresponds to an odd number of such permutations of pairs of nuclei, the total wavefunction of the tubular rotor must change sign upon application of g_p. Since the total wavefunction can be written as product of spatial times nuclear spin wavefunctions, we have

$$g_p\,\Psi_{total} = g_p\,\Psi_{spatial} * \Psi_{nu.spin} = g_p\,\Psi_{spatial} * g_p\,\Psi_{nu.spin}$$

$$= -\Psi_{total} = -\Psi_{spatial} * \Psi_{nu.spin}. \qquad (5)$$

As a test, it is gratifying that double application $g \circ g$ of the generator ($g: GM_1 \rightarrow GM_2$, $g: GM_2 \rightarrow GM_3$, cf. eqn. (1)) yields the same result as the first example ($g^2: GM_1 \rightarrow GM_3$). This is obvious for the rotation g_r of the wheel in the bearing, and also for the adjustment g_a of the bearing to the new position of the wheel. Likewise, the permutation g_p^2 (first example, eqn. (3)) is obtained by double application of g_p (second example, eqn. (4)):

$$g_p^2 = g_p \,.\, g_p = (1\ 9\ 17\ 7\ 15\ 5\ 13\ 3\ 11)\ (2\ 10\ 18\ 8\ 16\ 6\ 14\ 4\ 12)\ (19\ 20)$$
$$.\ (1\ 9\ 17\ 7\ 15\ 5\ 13\ 3\ 11)\ (2\ 10\ 18\ 8\ 16\ 6\ 14\ 4\ 12)\ (19\ 20)$$
$$= (1\ 17\ 15\ 13\ 11\ 9\ 7\ 5\ 3)\ (2\ 18\ 16\ 14\ 12\ 10\ 8\ 6\ 4). \qquad (6)$$

Likewise, it is straightforward to construct the operators $g^k = \{g_r, g_a, g_p\}^k$ which generate the remaining GM_{k+1} from GM_1, k=3,4,…,18. For the rotations g_r^k, the result is already in eqn. (2), i.e. the molecular wheel has to be rotated in the

bearing by k*20 ° mod 360 °. The adjustment g_a^k requires the relaxation of the shape of the bearing to the new position of the molecular wheel, analogous to the two examples but now in general for the azimuthal angle 10 °+ k*20 °mod 360 °. The permutations g_p^k can be constructed recursively, $g_p^k = g_p \,.\, g_p^{k-1}$, starting from eqn. (6). The results g_p^k are listed in Table S1.

A special case in Table S1 is g_p^9 = (19 20), i. e. nine sequential applications of the generating permutation g_p are equivalent to the exchange of the nuclei of the molecular wheel, without any permutations of the nuclei of the bearing. This is confirmed in Figure S1. The subsequent permutations g_p^{10}, g_p^{11}, g_p^{12}, … have the same permutations of the nuclei of the bearing as g_p, g_p^2, g_p^3, …, but opposite permutations of the nuclei of the wheel. This shows that whenever the wheel completes a half cycle, the nuclei of the bearing make a full cycle of permutations.

The adjustment g_a (in general: g_a^k) of the bearing and the permutation g_p (in general: g_p^k) of the nuclear labels imply that the original coordinates of the nuclei in GM_1 are replaced by new ones in GM_2 (in general: GM_{k+1}); the details are in SI VI.

The effect of the generator g = {g_r, g_a, g_p} is equivalent another generator $\tilde{g}$ which comprises the overall rotation (R) of the reference GM_1 by 20 °+ 180 °= 200 °combined with the permutation (19 20) of the nuclei of the wheel, cf. Figure 1. Symbolically, this alternative set of operations may be written as

the generator $\tilde{g}$ = {$\tilde{g}_R$, $\tilde{g}_{(19\ 20)}$},

- $\tilde{g}_R : \varphi_R \rightarrow (\varphi_R + 20\ ° + 180\ °) \bmod 360\ °$
- $\tilde{g}_{(19\ 20)}$ = (19 20). (7)

Irrespective of the same effects of the two generators g and $\tilde{g}$, they are entirely different, i.e. they involve rather small and rather large amplitude motions of the nuclei, respectively. Moreover, g requires significant permutations of all boron nuclei, eqn. (3), whereas $\tilde{g}$ invokes permutations of the labels of the nuclear wheel, only. The effects of the operators g^k (but not the mechanisms!) are the same as $\tilde{g}^k$ i.e. rotation of GM_1 by k*200 ° (mod 360 °) combined with k-fold exchanges $(19\ 20)^k$ of the nuclei 19,20 of the wheel.

SI II: The generation of all transition states of the oriented tubular rotor La-[B_2@B_{18}]-La

The generation of all transition states of the tubular molecular rotor La-[B_2@B_{18}]-La is entirely analogous to the generation of all global minimum structures, cf. SI I. Thus starting from the reference $TS_{18,1}$, one can generate the cyclic sequence $TS_{1,2}$, $TS_{2,3}$,…,$TS_{17,18}$ of all TSs by sequential applications of the generator g which comprises the familiar three operations, g = {g_r, g_a, g_p), eqn. (4). That means g, g^2, …, g^{17} and e= g^{18} transform $TM_{18,1}$ into $TS_{1,2}$, $TS_{2,3}$,…,$TS_{17,18}$ and then back to $TS_{18,1}$, symbolically

$$\begin{aligned} g \quad &: TS_{18,1} \rightarrow TS_{1,2},\ TS_{1,2} \rightarrow TS_{2,3},\ \ldots,\ TS_{16,17} \rightarrow TS_{17,18},\ TS_{17,18} \rightarrow TS_{18,1} \\ g^k \quad &: TS_{18,1} \rightarrow TS_{k,k+1} \text{ for } k=1,2,\ldots,17, \\ e = g^{18} &: TS_{18,1} \rightarrow TS_{18,1}, \end{aligned} \qquad (8)$$

analogous to eqn. (1) for the GMs. The same effects (but different mechanisms!) are achieved by sequential applications of the generator $\tilde{g}$ = {$\tilde{g}_R$, $\tilde{g}_{(19\ 20)}$}, eqn. (7),

$$\begin{aligned} \tilde{g} \quad &: TS_{18,1} \rightarrow TS_{1,2},\ TS_{1,2} \rightarrow TS_{2,2},\ \ldots,\ TS_{16,17} \rightarrow TS_{17,18},\ TS_{17,18} \rightarrow TS_{18,1} \\ \tilde{g}^k \quad &: TS_{18,1} \rightarrow TS_{n,n+1} \text{ for } k=1,2,\ldots,17. \\ e = \tilde{g}^{18} &: TS_{18,1} \rightarrow TS_{18,1}. \end{aligned} \qquad (9)$$

The azimuthal angle of the reference $TS_{18,1}$ is $\varphi_{18,1}$ = 0 °, halfway between the angles φ_{18} = 350° and φ_1 = 10 ° of the neighboring GM_{18} and GM_1. As consequence, the azimuthal angles $\varphi_{1,2}$, …, $\varphi_{17,18}$ of the molecular wheel in $TS_{1,2}$, …., $TS_{17,18}$ are equal to 20°, …, 340 °.

The reference $TS_{18,1}$ and the resulting $TS_{1,2}$, …, $TS_{17,18}$ are illustrated in Figures 1 and S2.

SI III: The cyclic molecular symmetry group C_{18}(M) of the oriented tubular rotor La-[B_2@B_{18}]-La

The set of the identity operator e, the generator g and sixteen multiple (k=2, 3, …, 16, 17) applications of g (cf. SI5) establishes the cyclic molecular symmetry group

$$C_{18}(M) = \{e, g, g^2, g^3, \ldots, g^{17}\} \quad (10)$$

of the oriented tubular rotor La-[B_2@B_{18}]-La, with $g^k \cdot g^{k'} = g^{(k+k') \bmod 18}$. Its order is N = 18. According to Ref. 24, it can be represented by the cyclic graph Gr(18,2) for 18 connected global minima and 2 energy pathways leading to each minimum. For comparison, the order of the full permutation-inversion (FPI) group is 2!*20!*2. Each global minimum has C_{2h} symmetry, with order 4. Accordingly, the total number of all global minima of the FPI group is N_{FPI} = 2!*20!*2/4 = 20!. As consequence, at low energies, its graph Gr_{FPI}(20!, 2) is split into $k=N_{FPI}/N$ = 20! /18 disconnected graphs Gr(18,2). The cyclic molecular symmetry group C_{18}(M) is isomorphic to the corresponding groups for the rotations of the molecular wheel in the bearing, for the adjustment of the bearing to the new position of the wheel, and for the permutations of the nuclear labels,

$$C_{18}(M)_r = \{e_r, g_r, g_r^2, g_r^3, \ldots, g_r^{17}\}$$

$$C_{18}(M)_a = \{e_a, g_a, g_a^2, g_a^3, \ldots, g_a^{17}\}$$

$$C_{18}(M)_p = \{e_p, g_p, g_p^2, g_p^3, \ldots, g_p^{17}\}. \quad (11)$$

The four group theorems (completeness of the group, existence of the identity e, existence of the inverse element g^{18-k} of g^k, and the associative law) are satisfied obviously. Moreover, the group operations commute, $g^k \cdot g^{k'} = g^{k'} \cdot g^k$, i. e. the cyclic molecular symmetry group C_{18}(M) is Abelian.

The cyclic molecular symmetry group C_{18}(M) is also isomorphic to the group

$$\tilde{C}_{18}(M) = \{\tilde{e}, \tilde{g}, \tilde{g}^2, \tilde{g}^3, \ldots, \tilde{g}^{17}\} \quad (12)$$

of the combined operations, eqn. (7), but again, the present g and the alternative $\tilde{g}$ are entirely different.

The general properties of cyclic groups imply that the present cyclic group C_{18}(M) has 18 one-dimensional irreducible representations (IRREPs) Γ_n, n=0,1,2,…,17 with characters [13]

$$\chi^{\Gamma n}(g^k) = \epsilon^{nk}, \quad \epsilon=\exp(-2\pi i/18), \quad n,k = 0,1,2,\ldots,17. \quad (13)$$

The corresponding symmetry projection operators for IRREP Γ_n are

$$P^{\Gamma n} = (1/18)\ \Sigma_{k=0}{}^{17}\ \chi^{\Gamma n}(g^k)^*\ g^k\ \ , n = 0,1,2,\ldots,17. \qquad (14)$$

Analogous expressions (with g replaced by $\tilde{g}$ etc) hold for the other isomorphic cyclic molecular symmetry groups, particularly for $\tilde{C}_{18}(M)$ and also for $C_{18}(M)_r$, $C_{18}(M)_a$ and $C_{18}(M)_p$.

The combined operations $\tilde{g}$, eqn. (7), commute with the molecular Hamiltonian H_{mol}, because the molecular energies do not depend, neither on the molecular orientation, nor on the exchange of the labels of nuclei 19 and 20. Likewise, the combined operation g, eqn. (4), commutes with H_{mol} – after all, the effects of g and $\tilde{g}$ are equivalent. Moreover, repeated applications g^k of g (or $\tilde{g}^k$ of $\tilde{g}$) commute with H_{mol}. As consequence, the symmetry projection operators (14) of $C_{18}(M)$ (or analogous symmetry projection operators of $\tilde{C}_{18}(M)$) commute with H_{mol},

$$[H_{mol}, g^k] = [H_{mol}, P^{\Gamma n}] = 0. \qquad (15)$$

The molecular eigenstates are characterized, therefore, not only by their eigenenergies, but they can also be assigned to specific IRREPs Γ_n of $C_{18}(M)$, with characters $\chi^{\Gamma n}(g^k)$. This "unified" assignment is more general compared to the assignments of the IRREPs a_g, b_g, a_u and b_u of the "local" molecular point groups C_{2h} of the individual GMs. For example, the normal mode v_8^{GM} can be assigned to IRREP b_g for the C_{2h} symmetry of GM_1, but it cannot be assigned to any IRREP of the C_{2h} symmetries of the other GMs, because they have different local symmetry elements e. g. the C_2 axes of the GMs have different orientations. In contrast, eqn. (15) implies that one can assign the vibrational modes of La-[B_2@B_{18}]-La to the IRREPs Γ_n of the molecular symmetry group $C_{18}(M)$, and these modes comprise all GMs. An important example, namely for the "unified" extension of all "local" normal modes v_8^{GM} of all GMs to the corresponding "unified" vibrational modes with IRREPs Γ_n of the molecular symmetry group $C_{18}(M)$ of La-[B_2@B_{18}]-La, will be presented in SI IV.

SI IV: Solution of the Schrödinger equation for the model of the rotating molecular wheel in the pseudo-rotating bearing of the oriented tubular rotor La-[B_2@B_{18}]-La

The rotation of the molecular wheel (B_2) along the angle φ in the oriented pseudo-rotating tubular bearing (B_{18}) of the rotor La-[B_2@B_{18}]-La, with the two

La nuclei as spectators on the cylindrical axis, is described quantum mechanically by means of the time independent Schrödinger equation (TISE)

$$H(\varphi)\,\Psi_m(\varphi) = E_m\,\Psi_m(\varphi). \qquad (16)$$

The model Hamiltonian

$$H(\varphi) = T(\varphi) + V(\varphi) \qquad (17)$$

in eqn. (16) accounts for the kinetic and potential energies of the rotational/pseudo-rotational motions. Specifically,

$$T(\varphi) = l_\varphi^2/(2\,I_{eff}) \qquad (18)$$

with effective moment of inertia I_{eff}, as derived in SI V, and with angular momentum operator

$$l_\varphi = -\,i\,\hbar\,d/d\varphi \qquad (19)$$

for the rotation of the molecular wheel in the oriented pseudo-rotating tubular bearing. The cyclic model potential $V(\varphi) = 0.5 * V_b\,[1 + \cos(18\,\varphi)]$ with its eighteen equivalent potential minima supporting eighteen equivalent global minimum structures, separated by eighteen equivalent transition states, is shown in Figure 3.

The TISE (16) is solved for the rotational/pseudo-rotational eigenenergies E_m and eigenfunctions $\Psi_m(\varphi)$ of the eigenstates labeled m = 0,1,2,…, with cyclic boundary conditions

$$\Psi_m(\varphi=0) = \Psi_m(\varphi=2\pi), \qquad (20)$$

by means of the methods which have been developed for planar boron rotors such as B_{11}^- or B_{13}^+, cf. Refs. [14, 16]. Suffice it here to say that the eigenfunctions are expanded in terms of normalized basis functions $(1/\sqrt{2\pi})\exp(i\,l\,\varphi)$ which satisfy the boundary conditions (20) automatically,

$$\Psi_m(\varphi) = \Sigma_{l=lmin}^{lmax}\,c_{ml}\,(1/\sqrt{2\pi})\,\exp(i\,l\,\varphi). \qquad (21)$$

In principle, the sum $\Sigma_{l=lmin}^{lmax}$ should run from $l_{min} = -\infty$ to $l_{max} = +\infty$. In practice, converged results are obtained by truncating the sum to lower and upper

boundaries l_{min} = 360 and l_{max} = 360. The expansion (21) allows to transform the TISE (16) into the algebraic version

$$\mathbf{H}\,\mathbf{c}_m = \mathbf{c}_m\,E_m \qquad (22)$$

with the vector $\mathbf{c}_m$ of the expansion coefficients c_{ml}. The notations are also adapted from Refs. [14, 16]; in particular, the ground state is denoted by the quantum number m=0, and the quantum numbers m increase with energy E_m.

The resulting eigenenergies E_m with quantum numbers m=0-53 are listed in Table S3. This Table is for the complete set of eigenstates with energies below the potential barrier V_b. The energy levels for six examples with quantum numbers m = 0, 17, 18, 35, 36, 53 are illustrated in Figure S5. Apparently, these 54 energies are arranged in three narrow "bands" which are separated from each other by rather large energy gaps. The bands may be labeled by "band energy quantum numbers" l=0,1,2 (see also eqn. (23) below). Each energy band has eighteen rotational/pseudo-rotational eigenstates, i. e. the lowest band (l=0) has the states with energies E_m labeled m=0-17, the first excited band (l=1) is for m=18-35, and the second excited band (l=2) contains E_m labeled m=36-53. In each band, the lowest and highest energies are non-degenerate, whereas all other energies are doubly degenerate, e.g. $E_1 = E_2$, $E_3 = E_4$, …., $E_{15} = E_{16}$ for the lowest band (l=0), $E_{19} = E_{20}$, … , $E_{33} = E_{34}$ for band l=1 and $E_{37} = E_{38}$, … , $E_{51} = E_{52}$ for band l=2.

The six energy levels which are shown in Figure S5 are the lowest and highest non-degenerate levels of each band. The corresponding band widths of energy bands l=0,1 and 2 are equal to 0.035, 1.157 and 13.833 h c cm^{-1}, respectively, i. e. they grow rapidly with band energy quantum number l. The energy gaps between the centers of bands l = 0 and 1 is $\Delta E_{0,1}$ = (299.2 – 103.7 = 195.5) h c cm^{-1}. The corresponding energy gap between bands l=1 and 2 is $\Delta E_{1,2}$ = (467.5 – 299.2 = 168.3) h c cm^{-1}.

To interpret the results for the rotational/pseudo-rotational levels of the oriented tubular molecular rotor La-[B_2@B_{18}]-La, it is illuminating to consider first, for reference, the traditional picture of eighteen individual, non-interacting global minimum structures. In normal mode approximation, each of the GMs has its individual, non-interacting harmonic potential along the corresponding normal mode- here this is the selected b_g normal mode v^{GM} =8 with vibrational energy quantum $\hbar\omega_8^{GM}$ = 234.79 h c cm^{-1}. Accordingly, the eighteen GMs have corresponding eighteen degenerate eigenenergies. In harmonic approximation, the lowest three levels are $E_{l=0} = 0.5\ \hbar\omega_8^{GM}$ = 117.395 h c cm^{-1} , $E_{l=1} = 1.5\ \hbar\omega_8^{GM}$

= 352.185 h c cm^{-1} and $E_{l=2}$ = 2.5 $\hbar\omega_8^{GM}$ = 586.975 h c cm^{-1} , respectively- all below the potential barrier V_b.

In contrast with the traditional picture of eighteen non-interacting GMs, the unified quantum mechanical picture provides the anharmonic potential V(φ) with eighteen equivalent minima supporting eighteen equivalent GMs which interact. For the present energies below the potential barrier, the interaction is by tunneling. For didactic purpose, it is helpful to recall that tunneling in a double well potential with two minima for two GMs yields tunneling splitting of pairs of two degenerate levels of two individual GMs into a pairs of two non-degenerate levels of the interacting GMs. The tunneling splitting ΔE is related to the tunneling time T by the relation ΔE * T = h. The higher is the barrier, the more difficult is the tunneling, that means the longer is T and the narrower is ΔE. Excited states have higher energies closer to the potential barrier – this facilitates the tunneling, decreases the tunneling time T and hence increases the tunneling splitting ΔE. By analogy, the present potential with eighteen potential wells yields tunneling splitting of sets of eighteen degenerate levels of eighteen individual GMs into "bands" of (partially) non-degenerate levels of the interacting GMs. The tunneling splitting ΔE of the double well corresponds to the band width ΔE. The higher is the barrier, the more difficult is the tunneling, and the narrower is the band width ΔE. Excited states have higher energies closer to the potential barrier – this facilitates the tunneling, and increases the band width ΔE.

The gaps between the centers of the bands, $\Delta E_{0,1}$ = 195.5 h c cm^{-1} and $\Delta E_{1,2}$ = 168.3 h c cm^{-1}, of the interacting GMs are smaller than the reference vibrational quantum $\hbar\omega_8^{GM}$ = 234.79 h c cm^{-1} of the non-interacting GMs. There are two effects which contribute to this deviation: Firstly, the anharmonicity of the cosinusoidal potential implies the systematic decrease from the harmonic reference to $\Delta E_{0,1}$ and then further down to $\Delta E_{1,2}$. Secondly, the present choice of the approximate value of the effective moment of inertia, I_{eff} = 68.98 u$Å^2$, uses the value of the vibrational quantum $|\hbar\omega_i^{TS}|$ = 217.84 h c cm^{-1} of the normal mode v_i^{TS} of the transition state, instead of the higher value $\hbar\omega_8^{GM}$ = 234.79 h c cm^{-1} for the global minimum, cf. SI V.

The wavefunctions $\Psi_m(\varphi)$ which are shown in Figures 3 and S5 correspond to densities $\rho_m(\varphi) = |\Psi_m(\varphi)|^2$ which look the same in analogous domains of the eighteen potential wells of V(φ). This property holds for all eigenfunctions, also for those which are not shown in Figure S5. This means that the rotational/pseudo-rotational eigenstates of the model La-[B_2@B_{18}]-La represent equal populations of all eighteen equivalent GMs. In particular, the ground state

wavefunction $\Psi_{m=0}(\varphi)$ yields the density $\rho_{m=0}(\varphi)$ with eighteen equivalent maxima which are centered at the potential minima. This corresponds to the unified quantum mechanical structure of La-[B_2@B_{18}]-La which is illustrated in Figures 2 and S4. It has D_{9h} symmetry (instead of C_{2h} for the individual GMs).

From SI III, eqn. (15), it follows that the eigenstates of La-[B_2@B_{18}]-La should have two quantum numbers, namely for the energy and for the IRREP. By analogy with the results of Ref. [16], we can identify the previous quantum number m with two quantum numbers

$$m = (l,n) \tag{23}$$

where l denotes the energy band, and n labels the IRREP Γ_n of the cyclic group C_{18}(M). The IRREP Γ_n of the wavefunction $\Psi_m(\varphi) \equiv \Psi_{l,n}(\varphi)$ can be determined by means of the rule (cf. Ref. [15], eqn. (35))

$$\Gamma_n \leftrightarrow g\,\Psi_{l,n}(\varphi) = \epsilon^n \Psi_{l,n}(\varphi) \tag{24}$$

where ϵ=exp(- 2πi/18), cf. eqn. (13). For example, the wavefunctions which are shown in Figure S5 have

$$\begin{aligned}
&g\ \Psi_{m=0}(\varphi) \equiv g\,\Psi_{l=0,n=0}(\varphi) = \Psi_{l=0,n=0}(\varphi) = \epsilon^0 \Psi_{l=0,n=0}(\varphi) \leftrightarrow \text{IRREP } \Gamma_{n=0}\\
&g\ \Psi_{m=18}(\varphi) \equiv g\,\Psi_{l=1,n=9}(\varphi) = -\Psi_{l=1,n=9}(\varphi) = \epsilon^9 \Psi_{l=1,n=9}(\varphi) \leftrightarrow \text{IRREP } \Gamma_{n=9}\\
&g\ \Psi_{m=36}(\varphi) \equiv g\,\Psi_{l=2,n=0}(\varphi) = \Psi_{l=2,n=0}(\varphi) = \epsilon^0 \Psi_{l=2,n=0}(\varphi) \leftrightarrow \text{IRREP } \Gamma_{n=0}\\
&g\ \Psi_{m=53}(\varphi) \equiv g\,\Psi_{l=2,n=9}(\varphi) = -\Psi_{l=2,n=9}(\varphi) = \epsilon^9 \Psi_{l=2,n=9}(\varphi) \leftrightarrow \text{IRREP } \Gamma_{n=9}.
\end{aligned} \tag{25}$$

The assignments of the IRREPs of the eigenfunctions correlates with unique sets of non-zero coefficients in the expansion (21). For example, $\Psi_{m=0}$ and $\Psi_{m=36}$ have non-zero coefficients c_{ml}, for l = …, -36, -18, 0, 18, 36, …, whereas $\Psi_{m=18}$ and $\Psi_{m=53}$ have non-zero coefficients c_{ml}, for l = …,-27, -9, 9, 27, …

A complete list of all assignments of quantum numbers (23) is in Table S3. Accordingly, the eighteen eigenfunctions in each band have different IRREPs $\Gamma_{n=0}$, $\Gamma_{n=1}$, $\Gamma_{n=2}$,…., $\Gamma_{n=17}$. This has enormous consequences. Namely, according to eqns. (5) and (21), the total wavefunctions consist of the spatial wave functions $\Psi_{l,n}(\varphi)$ with IRREP Γ_n times nuclear spin wave functions $\Psi_{n'}$ with IRREP $\Gamma_{n'}$ where n' = 9 - n (for n = 0, 1,…, 9) or n' = 27 - n (for n = 10,11,…,17). This is the only way to satisfy the anti-symmetry of the total wave function, in accord with $g\,\Psi_{total} = \epsilon^n \epsilon^{9-n} \Psi_{total} = \epsilon^9 \Psi_{total} = -\Psi_{total}$ (or = $\epsilon^n \epsilon^{27-n} \Psi_{total} = \epsilon^{27} \Psi_{total}$ =

$-\Psi_{total}$), cf. eqn. (5). In each energy band, all wavefunctions belong, therefore, to different nuclear spin isomers. This implies that it is impossible to prepare superpositions of eigenfunctions which belong to the same energy band. As consequence, it is impossible to prepare wavefunctions which are localized in individual potential wells supporting individual GMs of La-[B_2@B_{18}]-La. Hence the oriented tubular molecular rotor La-[B_2@B_{18}]-La will never be observed as GM.

SI V: The effective moment of inertia I_{eff} of the rotation of the molecular wheel in the pseudo-rotating tubular bearing of the oriented rotor La-[B_2@B_{18}]-La

This chapter presents two complementary approaches to the effective moment of inertia I_{eff} which is used in the Schrödinger eqn. (16) (cf. eqns. (17)-(19)) for the calculation of the rotational/pseudo-rotational eigenstates of the oriented tubular rotor La-[B_2@B_{18}]-La. The two approaches involve different approximations. At the end, we shall compare the results.

The first approach considers the local dynamics of the tubular rotor when it passes through one of its global minimum structures, say GM_k at φ_k, or alternatively when it crosses one of its transition states, say $TS_{k,k+1}$ at $\varphi_{k,k+1}$. The potential energy curve at φ_k is approximately harmonic,

$$V(\varphi) \approx 0.5\ k^{GM}_{\varphi}\ (\varphi - \varphi_k)^2 \qquad (26)$$

with force constant

$$k^{GM}_{\varphi} = d^2V/d\varphi^2|_{\varphi=\varphi k} = 0.5 * 18^2 * V_b. \qquad (27)$$

This angular force constant is equal to the effective moment of inertia I_{eff} times the square of the frequency of the vibration which induces the path from GM_k to the neighboring $TS_{k-1,k}$ and $TS_{k,k+1}$ - in the present case, this is approximately the normal mode labeled v^{GM} =8 with $\hbar\omega_8^{GM}$ = 234.79 h c cm^{-1}, cf. Table S1,

$$k^{GM}_{\varphi} = I_{eff}^{GM} * (\omega_8^{GM})^2. \qquad (28)$$

Eqns. (27), (28) yield

$$I_{eff}^{GM} = k^{GM}_{\varphi} / (\omega_8^{GM})^2 = 0.5 * 18^2\ V_b / (\omega_8^{GM})^2 = 59.38\ u\text{Å}^2. \qquad (29)$$

Likewise, one can use the harmonic approximation of $V(\varphi)$ at a transition state, say $TS_{k,k+1}$ at $\varphi_{k,k+1}$

$$V(\varphi) \approx V_b - 0.5\, k^{TS}{}_{\varphi}\, (\varphi - \varphi_{k,k+1})^2 \qquad (30)$$

with negative force constant - $k^{TS}{}_{\varphi} < 0$ for the vibration which induces the path from $TS_{k,k+1}$ to the neighboring GM_k and GM_{k+1} – this is approximately the normal mode with imaginary frequency, $|\hbar\omega_i{}^{TS}|$ = 217.84 h c cm^{-1}. The corresponding result is

$$I_{eff}{}^{TS} = |k^{TS}{}_{\varphi}\,| / |\omega_i{}^{TS}|^2 = 0.5 * 18^2\, V_b / |\omega_i{}^{TS}|^2 = 68.98\ u\text{Å}^2. \qquad (31)$$

The results (29), (31) of this first approach suggest that I_{eff} is of the order 60-70 $u\text{Å}^2$.

The second approach calculates I_{eff} as sum of two contributions,

$$I_{eff} = I_{rot} + I_{psr}, \qquad (32)$$

where

$$I_{rot} = m_B\ (R_{19}{}^{GM})^2 + m_B\ (R_{20}{}^{GM})^2 \qquad (33)$$

is moment of inertia for the rotation of the wheel in the tubular bearing, and I_{psr} represents the effect of the pseudo-rotating nuclei of the bearing. The values of the radial nuclear coordinates of the boron nuclei of the wheel (i = 19, 20) yield

$$I_{rot} = 14.73\ u\text{Å}^2. \qquad (34)$$

Comparison of eqns. (29), (31) and (32), (34) reveals that I_{rot} is much smaller than I_{eff}. This suggests that the main contribution to the effective moment of inertia is not due to the rotation of the wheel, but to the pseudo-rotations of the 18 nuclei of the tubular bearing. For a rough estimate of I_{psr}, let us consider as a reference the limiting case where those nuclei move on smooth ellipsoidal pseudo-rotational paths. The coordinates listed in Table S2a yield radial variations 2 $\Delta R_{bearing}$ from 2.2426Å to 2.6476Å, angular variations $\Delta\varphi_{bearing}$ of ±1.9456°, and variations 2 $\Delta Z_{bearing}$ along z from 0.6743 Å to 0.8718 Å. By analogy with eqn. (33), we obtain the lower limit

$$I_{psr} > 18\ m_B * 4\ [\Delta R_{bearing}{}^2 + (R_{bearing}\ \Delta\varphi_{bearing})^2 + \Delta Z_{bearing}{}^2]$$

$$= 18 * 11.009 * 4 * [0.2025^2 + (2.3574*0.03396)^2 + 0.09875^2]\ u\text{Å}^2$$

$$= 18 * 11.009 * 4 * 0.05716\ u\text{Å}^2 = 45.31\ u\text{Å}^2. \quad (35)$$

The factor 4 accounts for the fact that a full rotational cycle of the the nuclei of the molecular wheel is associated with two pseudo-rotational cycles of the nuclei of the tubular bearing.

Comparison of eqns. (32), (34), (35) confirms that I_{eff} is dominated by the effects of the tubular bearing, not by the wheel. Most important for the pseudo-rotational contribution I_{psr} to I_{eff} are the radial motions of the nuclei of the bearing, whereas motions along φ and z are less efficient.

The reference value (14.73 + 45.31 = 60.04) $u\text{Å}^2$ of the sum $I_{rot} + I_{psr} = I_{eff}$ obtained by the second approach agrees well with the estimate $I_{eff}^{GM} = 59.38\ u\text{Å}^2$ derived by the first approach. It is, therefore, fair to say that the two approaches support each other, in spite of the different approximations. One should keep in mind, however, that the result of the second approach has been estimated for the ideal scenario of ellipsoidal pseudo-rotational paths. Figure S4 shows, however, that the paths have various turns. These cause retardations and accelerations which tend to increase the value of I_{eff}. Hence, we use the larger value $I_{eff}^{TS} = 68.98\ u\text{Å}^2$ as effective moment of inertia, cf. eqn. (31), whereas the estimate $I_{eff}^{GM} = 59.38\ u\text{Å}^2$ in eqn. (29) is considered as lower limit. The preference of the value of I_{eff} at the transition state is also confirmed by the corresponding vector arrow plots of the b_g normal mode at the TSs, which serve as better tangents to the pseudo-rotational path than the b_g mode at the GMs, cf. SI VIII.

SI VI: The nuclear coordinates of 18 equivalent global minimum structures and 18 transition states of the oriented tubular rotor La-[B_2@B_{18}]-La

This Section consists of six parts: **SI VI-A** specifies the nuclear coordinates of the reference global minimum structure GM_1 of the oriented tubular rotor La-[B_2@B_{18}]-La, in the laboratory frame. Here the nuclei are labeled by i = 1, …, 22, with i = 1, …, 18 for the boron nuclei of the tubular bearing, i = 19, 20 for the boron nuclei of the molecular wheel, and i = 21, 22 for the metal nuclei. **SI VI-B** has the nuclear coordinates of the boron nuclei of the wheel and of the metal nuclei, for all GM_k, k=1, …, 18. **SI VI-C** presents the nuclear coordinates of the eighteen nuclei of the tubular bearing for all GMs. Sub-sections **SI VI-D**, **SI VI-E** and **SI VI-F** are for the nuclear coordinates of the transition states, analogous to **SI VI-A**, **SI VI-B** and **SI VI-C** for the GMs. Specifically, **SI VI-D** has the nuclear coordinates of the reference $TS_{18,1}$, **SI VI-B** has the nuclear

coordinates of the boron nuclei of the wheel and of the metal nuclei, for all $TS_{k,k+1}$, k=18, 1, …, 17, and **SI VI-C** presents the nuclear coordinates of the eighteen nuclei of the tubular bearing for all TSs.

SI VI-A: The nuclear coordinates of the reference global minimum structure GM_1 of the oriented tubular rotor La-[B_2@B_{18}]-La

The nuclear coordinates of GM_1 of La-[B_2@B_{18}]-La are expressed conveniently in terms of cylindrical coordinates, in the laboratory frame. Accordingly, the boron nuclei of the wheel (i=19,20) are at (R_{19}^{GM} = 0.8177 Å, $\Phi_{19}^{GM} = \varphi_1$ = 10 °, Z_{19}^{GM} = -0.0017Å) and ($R_{20}^{GM} = R_{19}^{GM}$, $\Phi_{20}^{GM} = \Phi_{19}^{GM}$ + 180 °, $Z_{20}^{GM} = -Z_{19}^{GM}$). The nuclear coordinates of the two metal atoms (i=21,22) are (R_{21}^{GM} = 0 Å, Φ_{21}^{GM} = 0 °, Z_{21}^{GM} = 2.3981 Å) and (R_{22}^{GM} = 0 Å, Φ_{22}^{GM} = 0 °, $Z_{22}^{GM} = -Z_{21}^{GM}$), with arbitrary and irrelevant values of Φ_{21}^{GM} and Φ_{22}^{GM}. The cylindrical coordinates of the nuclei of the tubular bearing (i=1-18) are specified using the notation (R_i^{GM}, $\Phi_i + \Delta\Phi_i^{GM}$, Z_i^{GM}). Here we set Φ_1 = 10°, Φ_2 =30°, Φ_3 = 50°, …., Φ_{18} = 350°, with equal angular spacings of 20°; these angles Φ_i are called "the reference angles" – this is the abbreviated version of the explicit but lengthy term "the reference angles of the nuclei labeled i of the bearing of the reference GM_1". The $\Delta\Phi_i^{GM}$ are the deviations of the cylindrical angles from Φ_i. The fixation of the reference angles implies orientation of the scaffold of the bearing in the laboratory, except for the small deviations $\Delta\Phi_i^{GM}$. The azimuthal angle φ of the wheel with respect to the bearing can then be interpreted as the angle between the laboratory x-axis and the projection of the wheel on the x-y-plane.

The nuclear point group C_{2h} of GM_1 implies the following symmetry rules for the cylindrical coordinates (these rules are to be applied cyclically, that means modulo 18):

$R_{1+\lambda}^{GM} = R_{10-\lambda}^{GM} = R_{10+\lambda}^{GM} = R_{19-\lambda}^{GM}$, $\lambda = 0, \ldots, 4$;

(this means $R_1^{GM} = R_{10}^{GM}$, $R_2^{GM} = R_9^{GM} = R_{11}^{GM} = R_{18}^{GM}$, $R_3^{GM} = R_8^{GM} = R_{12}^{GM} = R_{17}^{GM}$, $R_4^{GM} = R_7^{GM} = R_{13}^{GM} = R_{16}^{GM}$, $R_5^{GM} = R_6^{GM} = R_{14}^{GM} = R_{15}^{GM}$.)

$\Delta\Phi_{1+\lambda}^{GM} = -\Delta\Phi_{10-\lambda}^{GM} = \Delta\Phi_{10+\lambda}^{GM} = -\Delta\Phi_{19-\lambda}^{GM}$, $\lambda = 0, \ldots, 4$;

(this means $\Delta\Phi_1^{GM} = \Delta\Phi_{10}^{GM} = 0°$, $\Delta\Phi_2^{GM} = -\Delta\Phi_9^{GM} = \Delta\Phi_{11}^{GM} = -\Delta\Phi_{18}^{GM}$, $\Delta\Phi_3^{GM} = -\Delta\Phi_8^{GM} = \Delta\Phi_{12}^{GM} = \Delta\Phi_{17}^{GM}$, $\Delta\Phi_4^{GM} = -\Delta\Phi_7^{GM} = \Delta\Phi_{13}^{GM} = -\Delta\Phi_{16}^{GM}$, $\Delta\Phi_5^{GM} = -\Delta\Phi_6^{GM} = \Delta\Phi_{14}^{GM} = -\Delta\Phi_{15}^{GM}$.)

and

$Z_{1+\lambda}^{GM} = -Z_{10-\lambda}^{GM} = -Z_{10+\lambda}^{GM} = Z_{19-\lambda}^{GM}$.

(this means $Z_1^{GM} = -Z_{10}^{GM}$, $Z_2^{GM} = -Z_9^{GM} = -Z_{11}^{GM} = Z_{18}^{GM}$, $Z_3^{GM} = -Z_8^{GM} = -Z_{12}^{GM} = Z_{17}^{GM}$, $Z_4^{GM} = -Z_7^{GM} = -Z_{13}^{GM} = Z_{16}^{GM}$, $Z_5^{GM} = -Z_6^{GM} = -Z_{14}^{GM} = Z_{15}^{GM}$.) (36)

The values of the cylindrical coordinates (R_i^{GM}, $\Delta\Phi_i^{GM}$, Z_i^{GM}) of the nuclei of the bearing of GM_1 of $La_2[B_2@B_{18}]$, i=1,…,18 are listed in Table S2a. The quantum chemical results are obtained at the PBE0[33] level with the 6-311+G(d)[34] basis set for B and the Stuttgart relativistic small-core pseudopotential for La[35,36] using the Gaussian 09 program.[37] The PBE0 results are in perfect agreement with the symmetry rule (36).

SI VI-B: The coordinates of the boron nuclei of the molecular wheel and of the metal nuclei for 18 equivalent global minimum structures of the oriented tubular rotor La-[B_2@B_{18}]-La

The cylindrical coordinates of the nuclei of the molecular wheel (i = 19, 20) and of the metal atoms (i = 21, 22) for arbitrary global minima GM_k (k = 1, …, 18) of La-[B_2@B_{18}]-La are

(R_{19}^{GM} = 0.8177 Å, $\Phi_{19}^{GM} = \varphi_k$ = -10 °+k*20 °, $Z_{19}^{GM} = (-1)^k$ * 0.0117 Å),
($R_{20}^{GM} = R_{19}^{GM}$, $\Phi_{20}^{GM} = \Phi_{19}^{GM}$ + 180 °, $Z_{20}^{GM} = -Z_{19}^{GM}$),
(R_{21}^{GM} = 0 Å, Φ_{21}^{GM} = 0 °, Z_{21}^{GM} = 2.3981 Å)
(R_{22}^{GM} = 0 Å, Φ_{22}^{GM} = 0 °, $Z_{22}^{GM} = -Z_{21}^{GM}$) for GM_k. (37)

In other words, when proceeding from GM_k to GM_{k+1}, then the azimuthal angle φ of the wheel increases by 20°, its diameter is robust, and the position of its nucleus 19 changes from slightly below (above) to slightly above (below) the x-y-plane, and *vice versa* for nucleus 20. The metal nuclei keep the same positions on the rotational axis, for all GMs.

SI VI-C: The coordinates of the boron nuclei of the tubular bearing for 18 equivalent global minimum structures of the oriented tubular rotor La-[B_2@B_{18}]-La

In Subsection **SI VI-A** we have specified the cylindrical coordinates of the boron nuclei labeled i=1, 2, …, 18 of the tubular bearing of the reference global

minimum structure $GM_{k=1}$ of the oriented La-[B_2@B_{18}]-La, see also Figures 1, S1 and Table S2a.

The goal of this Subsection **SI VI-C** is to derive the cylindrical coordinates of the boron nuclei in tubular bearings of all GMs. For this purpose, it is helpful (a) recognize that the nuclear coordinates of $GM_{k=1}$ are just a special case of a more general expression, ready for applications to all other GMs. Next we shall consider two examples (similar to Section **SI II**), namely (b) first the nuclear coordinates of GM_3 and (c) then those of GM_2. Finally (d) the compact general expression for the cylindrical coordinates of the nuclei i = 1, 2, …, 18 in the global minimum GM_k with arbitrary label i will be extrapolated.

(a) For $GM_{k=1}$, the cylindrical coordinates of the nuclei i=1, 2, …, 18 of the bearing can be written in compact notation as

$$G_{i,i} = (R_i^{GM}, \Phi_i + \Delta\Phi_i^{GM}, Z_i^{GM}). \quad (38)$$

(The letter "G" reminds of "G-lobal minimum".) It is rewarding that eqn. (38) may be recognized as special case of the general expression

$$\begin{aligned} G_{19-k+i,i} &= (R_{19-k+i}^{GM}, \Phi_i + \Delta\Phi_{19-k+i}^{GM}, (-1)^{k-1} Z_{19-k+i}^{GM}) \\ &\equiv (R_{1-k+i}^{GM}, \Phi_i + \Delta\Phi_{1-k+i}^{GM}, (-1)^{k-1} Z_{1-k+i}^{GM}). \end{aligned} \quad (39)$$

The first subscript 19-k+i of $G_{19-k+i,i}$ depends on k and i, where the label k specifies the GM (here k=1 for $GM_{k=1}$), and i specifies the reference angle Φ_i of the nucleus of the bearing. The subscripts "19-k+i" or "1-k+i" are applied modulo 18, that means in a cyclic manner, (19-k+i) mod 18 = (1-k+i) mod 18. The second subscript i of $G_{19-k+i,i}$ specifies the reference angle Φ_i.

(b) As explained for the first example which has been discussed in Section **SI II**, $GM_{k=3}$ can be generated by rotation $g_r^{\sim 2}$ of $GM_{k=1}$ by 2*20 °(+ 2*180 °). This way, the labels i=1,2,3,4,…,18 of the nuclei in GM_1 are replaced by the labels 17,18,1,2,…,16 in $GM_{k=3}$, respectively, cf. Figure 1. As consequence, for example the cylindrical coordinates $G_{1,1}^{GM} = (R_1^{GM}, \Phi_1 + \Delta\Phi_1^{GM}, Z_1^{GM})$ of the nucleus i=1 in GM_1 at the reference angle $\Phi_{i=1}$ are replaced by the coordinates $G_{17,1}^{GM} = (R_{17}^{GM}, \Phi_1 + \Delta\Phi_{17}^{GM}, Z_{17}^{GM})$ of the nucleus 17 in $GM_{k=3}$. It is rewarding that this can be rewritten in terms of the general expression (39) as $G_{19-k+1,i=1} = (R_{19-k+1}^{GM}, \Phi_{i=1} + \Delta\Phi_{19-k+1}^{GM}, (-1)^{k-1} Z_{19-k+1}^{GM})$ for k=3. Likewise, the nuclei i = 17, 18, 1, 2, …, 16 in $GM_{k=3}$ have new coordinates $G_{19-k+i,i} = (R_{19-k+i}^{GM}, \Phi_i + \Delta\Phi_{19-k+i}^{GM}, (-1)^{k-1} Z_{19-k+i}^{GM})$.

(c) According to the second example which has been discussed in Section **SI II**, $GM_{k=2}$ can be generated by rotation $g_R\tilde{}$ of $GM_{k=1}$ by 20 °+180 ° = 200 °, accompanied with the permutation $g_{(19\,20)}\tilde{}$ of the nuclear labels of the wheel. This way, the labels i = 1, 2, …., 10, 11, …,18 of the nuclei in GM_1 are replaced by the labels 9, 10, …, 18, 1, …, 8 in $GM_{k=2}$, respectively, cf. Figure 1. As consequence, the cylindrical coordinates $G_{1,1} = (R_1^{GM}, \Phi_1 + \Delta\Phi_1^{GM}, Z_1^{GM})$ of the nucleus i=1 in GM_1 at the reference angle $\Phi_{i=1}{}^{GM}$ are replaced by the coordinates $(R_9^{GM}, \Phi_1 + \Delta\Phi_9^{GM}, Z_9^{GM})$ of the nucleus 9 in $GM_{k=2}$. The symmetry relations (36) imply, however, that these coordinates are the same as $(R_{18}^{GM}, \Phi_1 + \Delta\Phi_{18}^{GM}, - Z_{18}^{GM})$. Again, it is rewarding that this can be rewritten in terms of the general expression (39) as $G_{19\text{-}k+1.i} = (R_{19\text{-}k+1}^{GM}, \Phi_{i=1} + \Delta\Phi_{19\text{-}k+1}^{GM}, (-1)^{k-1}\, Z_{19\text{-}k+1}^{GM})$ for k=2. Likewise, the nuclei i = 9, 10, …, 18, 1, …, 8 in $GM_{k=2}$ at the reference angles $\Phi_1, \Phi_2, …., \Phi_{10}, \Phi_{11}, …, \Phi_{18}$ have new coordinates $G_{19\text{-}k+i.i} = (R_{19\text{-}k+i}^{GM}, \Phi_i + \Delta\Phi_{19\text{-}k+i}^{GM}, (-1)^{k-1}\, Z_{19\text{-}k+i}^{GM})$.

(d) Extrapolation of the results for the examples (a) - (c) to all other global minimum structures yields the general result, eqn. (39). The corresponding cylindrical coordinates of all the nuclei in the bearings of all GMs are listed in Table S2b.

The compact rule (39) has been derived by means of various results of the previous Sections **SI II** and **SI VI-A.** In particular, GM_k is generated by application of the operator $g^{\tilde{}k-1}$, equivalent to (but different from) g^{k-1}, on the reference GM_1. This implies the permutation $g_p{}^{k-1}$ of the nuclear labels 1, 2, 3, …, 18 in the bearing of GM_1 to new labels in GM_k, as documented in Figures 1, SI1and also in Tables S1, S2a. The symmetry relations (36) which are based on the C_{2h} symmetry of the reference GM_1 of La-[B_2@B_{18}]-La then allow to express the new cylindrical coordinates of the nuclei at the reference angles Φ_i of the tubular bearings of all GM_k by the compact rule (39).

SI VI-D: The nuclear coordinates of the reference transition state $TS_{18,1}$ of the oriented tubular rotor La-[B_2@B_{18}]-La

The nuclear coordinates of $TS_{18,1}$ (like those of GM_1) of La-[B_2@B_{18}]-La are expressed conveniently in terms of cylindrical coordinates. Accordingly, the boron nuclei of the wheel (i=19,20) are at (R_{19}^{TS} = 0.8182 Å, $\Phi_{19}^{TS} = \varphi_{18,1}$ = 0 °, Z_{19}^{TS} = 0 Å) and ($R_{20}^{TS} = R_{19}^{TS}$, $\Phi_{20}^{TS} = \Phi_{19}^{TS}$ + 180 °, Z_{20}^{TS} = 0 Å). The nuclear coordinates of the two metal atoms (i=21,22) are (R_{21}^{TS} = 0 Å, Φ_{21}^{TS} = 0 °, Z_{21}^{TS}

= 2.3916 Å) and (R_{22}^{TS} = 0 Å, Φ_{22}^{TS} = 0 °, Z_{22}^{TS} = $-Z_{21}^{TS}$), with arbitrary and irrelevant values of Φ_{21}^{TS} and Φ_{22}^{TS}.

The cylindrical coordinates of the nuclei of the bearing (i=1-18) are specified using the notation (R_i^{TS}, $\Phi_i + \Delta\Phi_i^{TS}$, Z_i^{TS}), with the same "reference angles" Φ_i as for GM_1. The $\Delta\Phi_i^{TS}$ are the deviations of the cylindrical angles from Φ_i. Note that the labels i=1-18 for the reference angles coincide with the labels of the nuclei i=1-18 in the reference global minimum structure GM_1. This coincidence yields compact expressions for the coordinates of all nuclei of all transition states, analogous to those for the global minima, and this is the reason for identifying the nuclear labels of $TS_{18,1}$ with those of GM_1. For comparison, the alternative choice namely identifying the nuclear labels of $TS_{18,1}$ with those of GM_{18} would not allow this formal analogy.

The nuclear point group C_{2h} of $TS_{18,1}$ implies the following symmetry rules for the cylindrical coordinates (these rules are applied cyclically, that means modulo 18):

$R_{5-\lambda}^{TS} = R_{5+\lambda}^{TS} = R_{14-\lambda}^{TS} = R_{14+\lambda}^{TS}$, $\lambda = 0, \ldots, 4$;

(this means $R_5^{TS} = R_{14}^{TS}$, $R_4^{TS} = R_6^{TS} = R_{13}^{TS} = R_{15}^{TS}$, $R_3^{TS} = R_7^{TS} = R_{12}^{TS} = R_{16}^{TS}$, $R_2^{TS} = R_8^{TS} = R_{11}^{TS} = R_{17}^{TS}$, $R_1^{TS} = R_9^{TS} = R_{10}^{TS} = R_{18}^{TS}$.)

$\Delta\Phi_{5-\lambda}^{TS} = -\Delta\Phi_{5+\lambda}^{TS} = \Delta\Phi_{14-\lambda}^{TS} = -\Delta\Phi_{14+\lambda}^{TS}$, $\lambda = 0, \ldots, 4$;

(this means $\Delta\Phi_5^{TS} = \Delta\Phi_{14}^{TS} = 0°$, $\Delta\Phi_4^{TS} = -\Delta\Phi_6^{TS} = \Delta\Phi_{13}^{TS} = -\Delta\Phi_{15}^{TS}$, $\Delta\Phi_3^{TS} = -\Delta\Phi_7^{TS} = \Delta\Phi_{12}^{TS} = -\Delta\Phi_{16}^{TS}$, $\Delta\Phi_2^{TS} = -\Delta\Phi_8^{TS} = \Delta\Phi_{11}^{TS} = -\Delta\Phi_{17}^{TS}$, $\Delta\Phi_1^{TS} = -\Delta\Phi_9^{TS} = \Delta\Phi_{10}^{TS} = -\Delta\Phi_{18}^{TS}$.)

and

$Z_{5-\lambda}^{TS} = Z_{5+\lambda}^{TS} = -Z_{14-\lambda}^{TS} = -Z_{14+\lambda}^{TS}$, $\lambda = 0, \ldots, 4$.

(this means $Z_5^{TS} = -Z_{14}^{TS}$, $Z_4^{TS} = Z_6^{TS} = -Z_{13}^{TS} = -Z_{15}^{TS}$, $Z_3^{TS} = Z_7^{TS} = -Z_{12}^{TS} = -Z_{15}^{TS}$, $Z_2^{TS} = Z_8^{TS} = -Z_{11}^{TS} = -Z_{17}^{TS}$, $Z_1^{TS} = Z_9^{TS} = -Z_{10}^{TS} = -Z_{18}^{TS}$.) (40)

The values of the cylindrical coordinates (R_i^{TS}, $\Delta\Phi_i^{TS}$, Z_i^{TS}) of the nuclei of the bearing of $TS_{18,1}$ of $La_2[B_2@B_{18}]$, I = 1, …, 18 are listed in Table S2b, adapted from Ref. [1]. They are in good but not in perfect agreement with the symmetry rule (40). For example, Table S2b has the value $\Delta\Phi_5^{TS}$ = 0.0012 ° instead of 0 °, or the value of $\Delta\Phi_4^{TS}$ is listed as 1.1927 °, whereas $-\Delta\Phi_6^{TS}$ = 1.1887 °, very close

to, but not the same as $\Delta\Phi_4^{TS}$. These small deviations are consequences of numerically imperfect rotations of the quantum chemical result for the TS in Ref. [1] to the present orientation, with the molecular wheel of $TS_{18,1}$ at $\varphi_{19} = 0\,°$ and with the cylindrical axis perpendicular to the x-y-plane. The deviations are below the graphical resolution of the Figures for the presentations of the subsequent results, however, so we consider them as negligible.

SI VI-E: The coordinates of the boron nuclei of the molecular wheel and of the metal nuclei for 18 equivalent transition states of the oriented tubular rotor La-[B_2@B_{18}]-La

The cylindrical coordinates of the boron nuclei of the wheel (I = 19, 20) and of the metal nuclei (I = 21, 22) of $TS_{k,k+1}$ (k=18,1,2,…,17) are

$$\begin{aligned}
&(R_{19}^{TS} = 0.8182\ \text{Å},\ \Phi_{19}^{TS} = k*20\ °,\ \ Z_{19}^{TS} = 0\ \text{Å}),\\
&(R_{20}^{TS} = R_{19}^{TS},\ \ \Phi_{20}^{TS} = \Phi_{19}^{TS} + 180\ °,\ Z_{20}^{TS} = 0\ \text{Å}),\\
&(R_{21}^{TS} = 0\ \text{Å},\ \ \Phi_{21}^{TS} = 0\ °,\ \ Z_{21}^{TS} = 2.3916\ \text{Å})\\
&(R_{22}^{TS} = 0\ \text{Å},\ \ \Phi_{22}^{TS} = 0\ °,\ \ Z_{22}^{TS} = -Z_{21}^{TS})\ \ \text{for } TS_{k,k+1},
\end{aligned} \tag{41}$$

compare with eqn. (38) for the GMs. In other words, all TSs have the molecular wheel in the x-y-plane, with robust diameter, and when proceeding from $TS_{k,k+1}$ to the next $TS_{k+1,k+2}$, then the azimuthal angle increases by 20 °. The metal nuclei keep the same positions on the rotational axis, for all TSs.

SI VI-F: The coordinates of the boron nuclei of the tubular bearing for 18 equivalent global transition states of the oriented tubular rotor La-[B_2@B_{18}]-La

The goal of this Subsection is to provide the cylindrical coordinates of all nuclei in all TSs. For this purpose, it is convenient to assign the label "k" to the transition state $TS_{k,k+1}$ (k=1,2,…,18 mod 18, e.g. k=18 for $TS_{18,1}$). This choice is of course somewhat arbitrary: it reminds of the "preceding" GM_k, instead of the alternative label "k+1" of the "next" GM_{k+1}. We choose the label "k" because it allows reaching the goal. The derivation is analogous to that presented in Subsection **SI VI-C** for the cylindrical coordinates of the nuclei in all GMs. In particular, it exploits the C_{2h} symmetry rules (40) for the coordinates of the reference $TS_{18,1}$, analogous to the C_{2h} symmetry rules (38) for the coordinates of the reference GM_1. As result, the cylindrical coordinates of the nuclei of the

tubular bearing of $TS_{k,k+1}$ at the reference angle Φ_i are given by the compact and general expression

$$T_{18-k+i.i} = (R_{18-k+i}^{TS}, \Phi_i + \Delta\Phi_{18-k+i}^{TS}, (-1)^k Z_{18-k+i}^{TS}) \equiv (R_{-k+i}^{TS}, \Phi_i + \Delta\Phi_{-k+i}^{TS}, (-1)^k Z_{-k+i}^{TS}) \quad (42)$$

with the subscripts modulo 18, analogous to eqn. (39) for GM_k. (The letter "T" reminds of "transition state".) Applications of this rule to all boron nuclei i = 1, 2, …, 18 in all TSs are listed in Table S2b

It is instructive to consider three examples of the rule (42) for the TSs, which correspond to the three applications (a), (b), (c) of the rule (39) to the GMs, as discussed in Subsection SI VI-C. (a) Gratifyingly, application of the rule (42) to the nuclei i=1,2,…,18 of the reference $TS_{18,1}$ (k=18) reproduces its cylindrical coordinates $T_{i,i} = (R_i^{TS}, \Phi_i + \Delta\Phi_i^{TS}, Z_i^{TS})$. (b) and (c): For the nuclei of the tubular bearing at the reference angle Φ_i of the next neighboring transition states $TS_{1,2}$ (k=1) and $TS_{2,3}$ (k=2), the rule (42) yields the coordinates $T_{17+i,i} = (R_{17+i}^{TS}, \Phi_i + \Delta\Phi_{17+i}^{TS}, - Z_{17+i}^{TS})$ and $(R_{16+i}^{TS}, \Phi_i + \Delta\Phi_{16+i}^{TS}, Z_{16+i}^{TS})$. The related permutations g_p and g_p^2 imply that the labels of the nuclei 1, 2, …, 18 of the "delivering" $TS_{18,1}$ are replaced in cyclic manner by (9,10,…,18,1,2,…,8) and by (17,18,1,2,…,16), as illustrated in Figure 1 and documented in Table S1.

SI VII: The rotating molecular wheel in the pseudo-rotating tubular bearing of the oriented rotor La-[B_2@B_{18}]-La

Until now, we have considered the generation of eighteen equivalent global minimum structures and eighteen equivalent transition states of the oriented La-[B_2@B_{18}]-La, by multiple applications of the generators g or g̃ to the reference GM_1 or to the reference $TS_{18,1}$, respectively. The generator g̃ invokes large amplitude motions of the individual nuclei of the tubular bearing, associated with permutation of the nuclear labels of the molecular wheel. For example, it rotates the rotor by 20 °+ 180 °about the cylindrical axis to its new position in the bearing of GM_2, cf. eqn. (7). In contrast, the generator g invokes small amplitude nuclear motions of the bearing, but these are associated with significant permutations of the nuclear labels, cf. eqn. (4). For example, it moves the nucleus of the bearing of GM_1 labeled i=1 from its position at cylindrical coordinates $G_{1,1}$ to the neighboring coordinates $G_{18,1}$ while permuting its label from 1 to 9, cf. Figure 1 and Tables S1, S2.

This Section introduces an equivalent generator $g^{\approx}$ which achieves the same effect as g or $\tilde{g}$, but with small amplitude motions of the nuclei of the bearing, and without any permutations of the nuclei. This generator $g^{\approx}$ implies a new mechanism for generating the cyclic sequence of alternating global minimum structures and transitions states, $TS_{18,1} \rightarrow GM_1 \rightarrow TS_{1,2} \rightarrow GM_2 \rightarrow \ldots \rightarrow TS_{17,18} \rightarrow GM_{18} \rightarrow TS_{18,1}$ of the tubular rotor, namely generation by rotating the molecular wheel in the pseudo-rotating tubular bearing. Specifically,

the generator $g^{\approx} = \{ g_r, g_{pr} \}$ consists of two operations, namely

- g_r: rotation of the molecular wheel in the tubular bearing by 20 °,

  g_r: $\varphi \rightarrow \varphi + 20°$

  (same as g_r for the generator **g**, eqn. (4)) and

- g_{pr} – this denotes the so-called "pseudo-rotation" of the nuclei of the bearing. Specifically, the nuclei at the reference angle Φ_i keep their label i, but the coordinates $G_{19-k+i,i} = (R_{19-k+i}^{GM}, \Phi_i + \Delta\Phi_{19-k+i}^{GM}, (-1)^{k-1} Z_{19-k+i}^{GM})$ in GM_k change to the coordinates $G_{19-(k+1)+i.i} = (R_{19-(k+1)+i}^{GM}, \Phi_i + \Delta\Phi_{19-(k+1)+i}^{GM}, (-1)^k Z_{19-(k+1)+i}^{GM})$ in GM_{k+1}, cf. eqn. (39)

  g_{pr} : $G_{19-k+i,i} \rightarrow G_{19-(k+1)+i.i}$ for $GM_k \rightarrow GM_{k+1}$, in particular

  g_{pr} : $G_{i,i} \rightarrow G_{17+i,i}$ for $GM_1 \rightarrow GM_2$.

  Repeated applications g_{pr}^k of g_{pr} change the coordinates $G_{i,i}$ in GM_1 to $G_{19-(k+1)+i,i}$ in $GM_{k+1,}$

  g_{pr}^k : $G_{i,i} \rightarrow G_{19-(k+1)+i,i}$ for $GM_1 \rightarrow GM_{k+1}$.

  Likewise, the coordinates $T_{18-k+I,i} = (R_{18-k+i}^{TS}, \Phi_i + \Delta\Phi_{18-k+i}^{TS}, (-1)^k Z_{18-k+i}^{TS})$ in $TS_{k,k+1}$ change to the coordinates $T_{18-(k+1)+i,i} = (R_{18-(k+1)+i}^{TS}, \Phi_i + \Delta\Phi_{18-(k+1)+i}^{TS}, (-1)^{k+1} Z_{18-(k+1)+i}^{TS})$ in $TS_{k+1,k+2}$, cf. eqn. (42),

  g_{pr} : $T_{18-k+i,i} \rightarrow T_{18-(k+1)+i,i}$ for $TS_{k,k+1} \rightarrow TS_{k+1,k+2}$, in particular

  g_{pr} : $T_{i,i} \rightarrow T_{17+i,i}$ for $TS_{18,1} \rightarrow TS_{1,2}$.

  Repeated applications g_{pr}^k of g_{pr} change the coordinates $T_{i,i}$ in $TS_{18,1}$ to

$T_{18\text{-}k+i,i}$ in $TS_{k,k+1}$

$$g_{pr}^{\,m} : T_{i,i} \rightarrow T_{18\text{-}k+i,i} \text{ for } TS_{18,1} \rightarrow TS_{k,k+1}. \quad (43)$$

The subscripts in eqn. (43) are applied modulo 18.

The equivalence of the generator $g^{\approx}$ and g or $\tilde{g}$ means that they achieve the same effects. Thus multiple applications $\tilde{g}^k$ or g^k of $\tilde{g}$ or g transfer the reference GM_1 and $TS_{18,1}$ into GM_{k+1} and $TS_{k,k+1}$, respectively, with corresponding permutations of the nuclear labels, and with the associated changes of the nuclear coordinates (39) and (42), as listed in Table S2b. For comparison, multiple applications $g^{\approx k}$ of $g^{\approx}$ transfer the reference GM_1 and $TS_{18,1}$ into the same GM_{k+1} and $TS_{k,k+1}$, respectively, with the same shifts of the nuclear coordinates, but without any nuclear permutations. These effects are equivalent, irrespective of the permutations or non-permutations of the nuclear labels of the bearing, because the boron nuclei are indistinguishable, i.e. their labels do not matter. What matters is that the GM_{k+1} and $TS_{k+1,k+2}$ are generated from the reference GM_1 and from $TS_{18,1}$ with eighteen boron nuclei at coordinates $G_{19\text{-}(k+1)+i,i}$ or $T_{18\text{-}(k+1)+i,i}$ in the bearing, respectively, irrespective of the nuclear labels. The suppression of any permutations of the nuclear labels means that the generator $g^{\approx}$ moves the nuclei of the bearing of the reference GM_1 such that they stay close to their reference angles Φ_i .

The effects of multiple applications $g^{\approx k}$ of $g^{\approx}$ operating on GM_1 or $TS_{18,1}$ are illustrated in the rainbow-colored Figures S1 and S2, respectively. For each step of the wheel from φ_k or $\varphi_{k,k+1}$ to φ_{k+1} or $\varphi_{k+1,k+2}$, the nuclei at the reference angles Φ_i in the bearing move from their positions at $G_{19\text{-}k+i,i}$ or $T_{18\text{-}m+n,n}$ to $G_{19\text{-}(k+1)+i,i}$ or $T_{18\text{-}(k+1)+i,i}$, respectively, without changing the nuclear labels. These nuclear motions in the bearing are called “pseudo-rotations”.

We shall now discuss some important properties of the model of the rotating wheel in the pseudo-rotating bearing. These properties are also documented in Figures 2 and S4, and they are confirmed by Table S2b when ignoring the labels of the nuclei at the reference angles Φ_i.

(a) Starting from the reference global minimum GM_1 or from the reference transition state $TS_{18,1}$, eighteen applications of the rotational-pseudo-rotational generator $g^{\approx}$ generate the cyclic sequences $GM_1 \rightarrow GM_2 \rightarrow \ldots \rightarrow GM_{18} \rightarrow GM_1$ or $TS_{18,1} \rightarrow TS_{1,2} \rightarrow \ldots \rightarrow TS_{17,18} \rightarrow TS_{18,1}$, respectively. At the same time, the nuclei of the molecular wheel move

along a full rotational cycle. The coordinates of the nuclei of the bearing at reference angle Φ_i move according to the cyclic sequences $G_{19-1+i,i} \rightarrow G_{19-2+i,i} \rightarrow \ldots \rightarrow G_{19-18+i,i} \rightarrow G_{19-1+i,i}$ or $T_{18+i,i} \rightarrow T_{18-1+i,i} \rightarrow \ldots \rightarrow T_{18-17+i,i} \rightarrow T_{18+i,i}$, respectively. The symmetry relations (36) and (40) – which are consequences of the C_{2h} symmetries of the reference GM_1 and $TS_{18,1}$ – imply that these sequences are periodic, with period 9, i.e.

$$G_{19-k+i,i} = G_{19-(k+9)+i,i},$$

$$T_{18-k+i,i} = T_{18-(k+9)+i,i}.$$

or

$$\begin{aligned} & G_{19-1+i,i} \rightarrow G_{19-2+i,i} \rightarrow \ldots \rightarrow G_{19-9+i,i} \rightarrow G_{19-10+i,i} \\ = & G_{19-10+i,i} \rightarrow G_{19-11+i,i} \rightarrow \ldots \rightarrow G_{19-18+i,i} \rightarrow G_{19-1+i,i}, \end{aligned}$$

$$\begin{aligned} & T_{18+i,i} \rightarrow T_{18-1+i,i} \rightarrow \ldots \rightarrow T_{18-8+i,i} \rightarrow T_{18-9+i,i} \\ = & T_{18-9+i,i} \rightarrow T_{18-10+i,i} \rightarrow \ldots \rightarrow T_{18-17+i,i} \rightarrow T_{18-18+i,i}. \end{aligned} \qquad (44)$$

Each of the cyclic sequences (44) accounts for one pseudo-rotational cycle of the nuclei of the bearing. This means that rotation of the molecular wheel by half a cycle (and then followed by the second half cycle to complete the full cycle) is associated with a full pseudo-rotational cycle (and then by the second full pseudo-rotational cycles) of the nuclei of the bearing.

(b) The concerted effect of eighteen pseudo-rotating nuclei of the bearing appears *as if* the bearing rotates, even though it does not rotate. This is rationalized by the equivalence of the two generators, $g^{\approx}$ and $\tilde{g}$. The property (a) then implies that when the wheel rotates by half a cycle (and then by another half cycle to complete the full cycle), the bearing appears *as if* it rotates by a full cycle (and then by the second full cycle).

(c) The cylindrical coordinates of the nuclei at neighboring reference angles Φ_i and Φ_{i+1} are related to each other,

$$\begin{aligned} & (R_{19-k+i}{}^{GM}, \Phi_i + \Delta\Phi_{19-k+i}{}^{GM}, (-1)^{k-1} Z_{19-k+i}{}^{GM}) \\ = & (R_{19-(k+1)+(i+1)}{}^{GM}, \Phi_{i+1} - 20\,^\circ + \Delta\Phi_{19-(k+1)+(i+1)}{}^{GM}, \\ & \qquad -(-1)^k Z_{19-(k+1)+(i+1)}{}^{GM}). \end{aligned}$$

$$(R_{18-k+i}^{TS}\ ,\ \Phi_i\ +\ \Delta\Phi_{18-k+i}^{TS}\ ,\ (-1)^k\ Z_{18-k+i}^{TS})$$

$$=(R_{18-(k+1)+(i+1)}^{TS},\ \Phi_{i+1} - 20\,^\circ + \Delta\Phi_{18-(k+1)+(i+1)}^{TS},\ -(-1)^{k+1}\ Z_{18-(k+1)+(i+1)}^{TS}). \quad (45)$$

From a mathematical point of view, these relations are trivial. But for the mechanism of the rotating wheel in the pseudo-rotating bearing, they have two consequences (d) and (e) which may appear less obvious:

(d) The pseudo-rotational sequences of the coordinates of the nuclei of the bearing (in brief: "the pseudo-rotational sequences") at all reference angles Φ_i "look the same", that means they can be mapped on each other by simple symmetry operations. Specifically, the pseudo-rotational sequence at Φ_i can be mapped on the sequence at the neighboring reference angle Φ_{i+1} by rotating it about the cylindrical axis by $\Phi_{i+1} - \Phi_i = 20\,^\circ$, together with reflection at the x-y-plane. As a consequence, the pseudo-rotational sequences at reference angles Φ_i with odd labels i = 1, 3, 5, …, 17 are rotated with respect to each other by $\Phi_{i+2} - \Phi_i = 40\,^\circ$, and they are all above the x-y-plane. In contrast, the pseudo-rotational sequences at reference angles Φ_i with even labels i = 2, 4, 6, ..., 18 are rotated with respect to those with odd labels i = 1, 3, 5, …, 17 by $\Phi_{i+1} - \Phi_i = 20\,^\circ$, together with the reflections which put them all below the x-y-plane.

(e) The pseudo-rotational sequences at neighboring reference angles Φ_{i+1} , Φ_i ($\Delta i=1$) are phase shifted to each other by $\Delta k=1$.

(f) An alternative version of writing eqn. (45) is

$$(R_{19-k+1}^{GM}\ ,\ \Phi_i\ +\ \Delta\Phi_{19-k+1}^{GM},\ (-1)^{k+1}\ Z_{19-k+1}^{GM})$$

$$= (R_{19-(k+i-1)+i}^{GM}\ ,\ \Phi_{i+1} - 20\,^\circ + \Delta\Phi_{19-(k+i-1)+i}^{GM}\ ,\ (-1)^{i-1}\ (-1)^{k+i}\ Z_{19-(k+i-1)+i}^{GM}).$$

$$(R_{18-k+1}^{TS}\ ,\ \Phi_i\ +\ \Delta\Phi_{18-k+1}^{TS}\ ,\ (-1)^k\ Z_{18-k+1}^{TS})$$

$$= (R_{18-(k+i-1)+i}^{TS},\ \Phi_{i+1} - 20\,^\circ + \Delta\Phi_{18-(k+i-1)+i}^{TS}\ ,\ (-1)^{i-1}\ (-1)^{k+i-1}\ Z_{18-(k+i-1)+i}^{TS}). \quad (46)$$

Again, this is mathematically trivial, but it has important consequences, namely it suffices to know the pseudo-rotational sequence of the cylindrical coordinates of the nucleus at reference angle $\Phi_{i=1} = 10°$. The corresponding sequences at reference angle Φ_i can then be generated by rotating them from $\Phi_{i=1}$ to $\Phi_{i,}$ with phase shifts by i-1 and with reflection at the x-y-plane for even numbers i. In practice, it thus suffices to know the pseudo-rotational sequence of the cylindrical coordinates of the nucleus at reference angle $\Phi_{i=1} = 10°$ - the coordinates at all other reference angle Φ_i can then be generated by means of the recipe (46).

(g) One can combine the pseudo-rotational sequences for the global minimum structures and for the transition states according to the cyclic sequence with alternating $TS_{k,k+1}$ and GM_k,

$$TS_{18,1} \rightarrow GM_1 \rightarrow TS_{1,2} \rightarrow GM_2 \rightarrow \ldots\ldots \rightarrow GM_{17} \rightarrow TS_{17,18} \rightarrow GM_{18} \rightarrow TS_{18,1}. \quad (47a)$$

This sequence is illustrated in Figures 2 and S4 which appears as a superposition of Figure S1 for the GMs and Figure S2 or the TSs. The cyclic sequence of the corresponding labels k (modulo 18) of $TS_{k,k+1}$ and GM_k is

$$k = 18(TS) \rightarrow 1(GM) \rightarrow 1(TS) \rightarrow 2(GM) \rightarrow \ldots\ldots \rightarrow 17(GM) \rightarrow 17(TS) \rightarrow 18(GM) \rightarrow 18(TS) \quad (47b)$$

It is convenient to map this cyclic sequence with “twins” of labels k to the cyclic sequence with “single” labels j (modulo 36)

$$j = 0 \rightarrow 1 \rightarrow 2 \rightarrow 3 \rightarrow \ldots\ldots \rightarrow 33 \rightarrow 34 \rightarrow 35 \rightarrow 36 (\equiv 0) \quad (47c)$$

The corresponding sequence of the azimuthal angle of the molecular wheel with respect to the oriented bearing is

$$\varphi_j\,[°] = 0 \rightarrow 10 \rightarrow 20 \rightarrow 30 \rightarrow \ldots \rightarrow 330 \rightarrow 340 \rightarrow 350 \rightarrow 360 \equiv 0 \quad (47d)$$

i.e. $\varphi_j = j * \Delta\varphi$, $\Delta\varphi = 360°/36 = 10°$.

The general expressions for the coordinates $R_{19-k+i,i}$ (eqn. (39)) and $T_{18-k+i,i}$ (eqn. (42)) for the nucleus in the bearing of La-[B_2@B_{18}]-La at reference angle Φ_i = 10°, 30°,50°,…,350° (i=1,2,3,…,18) yield the corresponding cyclic pseudo-rotational sequence of cylindrical coordinates

$$T_{i,i} \rightarrow G_{i,i} \rightarrow T_{17+i,i} \rightarrow G_{17+i,i} \rightarrow \ldots. \rightarrow G_{2+i,i} \rightarrow T_{1+i,i} \rightarrow G_{1+i,i} \rightarrow T_{i,i} \quad (47e)$$

In the explicit expressions (39) and (42), the cylindrical reference coordinates for the nuclei of the reference GM_1 and $TS_{18,1}$ can no be re-labeled by the single label j instead of the previous subscript k and superscripts GM or TS. For example, the corresponding cyclic reference sequence of the cylindrical radii

$$R_{k=18}^{TS} \rightarrow R_1^{GM} \rightarrow R_1^{TS} \rightarrow R_2^{GM} \rightarrow \ldots \rightarrow R_{17}^{GM} \rightarrow R_{17}^{TS} \rightarrow R_{18}^{GM} \rightarrow R_{18}^{TS} \quad (47f)$$

is then replaced by

$$R_{j=0} \rightarrow R_1 \rightarrow R_2 \rightarrow R_3 \rightarrow \ldots \rightarrow R_{33} \rightarrow R_{34} \rightarrow R_{35} \rightarrow R_{36\equiv 0} \quad (47g)$$

Likewise, the cyclic reference sequence of azimuthal deviations

$$\Delta\Phi_{k=18}^{TS} \rightarrow \Delta\Phi_1^{GM} \rightarrow \Delta\Phi_1^{TS} \rightarrow \Delta\Phi_2^{GM} \rightarrow \ldots \rightarrow \Delta\Phi_{17}^{GM} \rightarrow \Delta\Phi_{17}^{TS} \rightarrow \Delta\Phi_{18}^{GM} \rightarrow \Delta\Phi_{18}^{TS} \quad (47h)$$

is replaced by

$$\Delta\Phi_{j=0} \rightarrow \Delta\Phi_1 \rightarrow \Delta\Phi_2 \rightarrow \Delta\Phi_3 \rightarrow \ldots.. \rightarrow \Delta\Phi_{33} \rightarrow \Delta\Phi_{34} \rightarrow \Delta\Phi_{35} \rightarrow \Delta\Phi_{36\equiv 0}, \quad (47i)$$

and the cyclic reference sequence of Z-coordinates

$$Z_{k=18}^{TS} \rightarrow Z_1^{GM} \rightarrow Z_1^{TS} \rightarrow Z_2^{GM} \rightarrow \ldots \rightarrow Z_{17}^{GM} \rightarrow Z_{17}^{TS} \rightarrow Z_{18}^{GM} \rightarrow Z_{18}^{TS}$$

(47j)

is replaced by

$$Z_{j=0} \rightarrow Z_1 \rightarrow Z_2 \rightarrow Z_3 \rightarrow \ldots \rightarrow Z_{33} \rightarrow Z_{34} \rightarrow Z_{35} \rightarrow Z_{36\equiv 0}.$$

(47k)

An explicit list of the cylindrical reference coordinates (47g), (47i), (47k) depending on the azimuthal angle φ_j (47d) is presented in Table S2a.

(h) The previous symmetry relations (36) and (40) which depend on the C_{2h} symmetry of the reference GM_1 and $TS_{18,1}$ give rise to the following symmetry relations for the cylindrical coordinates labeled by the joint index j:

$$R_{1+\lambda} = R_{1-\lambda} = R_{19+\lambda} = R_{19-\lambda}$$

$$\Delta\Phi_{1+\lambda} = -\Delta\Phi_{1-\lambda} = \Delta\Phi_{19+\lambda} = -\Delta\Phi_{19-\lambda}$$

$$Z_{1+\lambda} = (-1)^{\lambda} Z_{1-\lambda} = -Z_{19+\lambda} = -(-1)^{\lambda} Z_{19-\lambda},\ \lambda = 0,1,2,... \qquad (48)$$

These rules are valid modulo (36). They can be verified by inspection of Table S2a.

(i) Using the joint index j = 0, 1, 2, 3, 4, … for the alternating TS and GM structures at the azimuthal angles $\varphi_j = j*10$ °of the wheel (B_2) with respect to the oriented bearing (B_{18}) of the tubular rotor La-[B_2@B_{18}]-La, the rules (39), (42) and (43) for the pseudo-rotational coordinates of the nucleus of the bearing at the reference angle $\Phi_{i=1} = 10$ °are translated into the pseudo-rotational sequence

$$(R_2, \Delta\Phi_2, Z_2) \rightarrow (R_1, \Delta\Phi_1, Z_1) \rightarrow (R_{0\equiv 36}, \Delta\Phi_{0\equiv 36}, -Z_{0\equiv 36}) \rightarrow (R_{35}, \Delta\Phi_{35}, -Z_{35}) \rightarrow (R_{34}, \Delta\Phi_{34}, Z_{34}) \rightarrow \ldots.$$

$$= (R_0, -\Delta\Phi_0, -Z_0) \rightarrow (R_1, -\Delta\Phi_1, Z_1) \rightarrow (R_2, -\Delta\Phi_2, Z_2) \rightarrow (R_3, -\Delta\Phi_3, -Z_3) \rightarrow (R_4, -\Delta\Phi_4, -Z_4) \rightarrow \ldots.$$

$$= (R_0, -\Delta\Phi_0, |Z_0|) \rightarrow (R_1, -\Delta\Phi_1, |Z_1|) \rightarrow (R_2, -\Delta\Phi_2, |Z_2|) \rightarrow (R_3, -\Delta\Phi_3, |Z_3|) \rightarrow (R_4, -\Delta\Phi_4, |Z_4|) \rightarrow \ldots.$$

$$\equiv (R_j, -\Delta\Phi_j, |Z_j|) \rightarrow,\ j = 0, 1, 2, 3, \ldots, 35, (36 \equiv 0). \qquad (49)$$

The first equation (49) is a consequence of the symmetry rules (36), (40). The minus sign in front of the deviations $-\Delta\Phi_j$ is in accord with the fact that the pseudo-rotation and the rotation of the wheel are both anti-clockwise. The second equation (49) is verified by inspection of Table S2b. It ensures that all positions of the nucleus at the reference angle $\Phi_1 = 10\,°$ are above the x-y-plane. According to the rule (47f), it suffices to know the pseudo-rotational sequence (49) at $\Phi_1 = 10\,°$. All other pseudo-rotational sequences at reference angles Φ_i can be generated from the rule (49) by application of the "trivial" eqn. (46) - in practice this means by rotation by $\Phi_i - \Phi_1$ together with alternating reflections at the x-y-plane. This yields the sequence (47e) of the coordinates of the nuclei of the bearing at $\Phi_i = 10°, 30°, 50°, \ldots, 350°$. The result is shown in Figures 2 and S1.

Figures 6a, 6b show the cyclic reference sequences of the cylindrical coordinates R_j, $-\Delta\Phi_j$ for the nucleus of the bearing at the reference angle $\Phi_1 = 10\,°$ versus the azimuthal angles φ_j of the molecular wheel. Figure 6c adds the cyclic sequence of the related reference Cartesian coordinates,

$$(X_j = R_j \cos(-\Delta\Phi_j), \quad Y_j = R_j \sin(-\Delta\Phi_j), |Z_j|), j=1,2,\ldots,36, (37\equiv 1). \tag{50}$$

Three-dimensional (3d) perspective views of selected pseudo-rotational paths are illustrated in the inserts of Figure S4a. Figure 8a shows the corresponding 2d projection (X_j, Y_j).

From the sequence of the pseudo-rotational cylindrical coordinates (R_j, $-\Delta\Phi_j$, $|Z_j|$) of the nucleus of the bearing at the reference angle $\Phi_{i=1}$ which are shown in Figures S6 and S7 one can generate the corresponding coordinates at the reference angles Φ_i, i=1, 2, …, 18 as explained in item f above, cf. eqn. (46). The result is shown in Figure S4a.

The corresponding cyclic sequence of the cylindrical coordinates of the two boron nuclei of the wheel (j=19,20) depend on φ_j, as follows: Their values of the radii alternate between the values for GM and TS,

$R_{19}(\varphi_j) = R_{20}(\varphi_j) = R_{19}^{GM} = 0.8177$ Å for j = 1, 3, 5, …., 33, 35 and

$$R_{19}(\varphi_j) = R_{20}(\varphi_j) = R_{19}^{TS} = 0.8182 \text{ Å for } j = 2, 4, 6, \ldots, 34, 36.$$

The azimuthal angles (modulo 360 °) are

$$\Phi_{19}(\varphi_j) = \varphi_j = j*\Delta\varphi,\ \Delta\varphi = 10°, \text{ and } \Phi_{20}(\varphi_j) = \Phi_{19}(\varphi_j) + 180\ °.$$

The Z-components are

$$Z_{19}(\varphi_j) = -\ Z_{20}(\varphi_j) = (-1)^{(j-1)/2}\ Z_{19}^{GM} = -(-1)^{(j-1)/2}\ 0.0177 \text{ Å}$$
$$\text{for } j = 1, 3, 5, \ldots., 33, 35 \text{ and}$$

$$Z_{19}(\varphi_j) = -\ Z_{20}(\varphi_j) = Z_{19}^{TS} = 0 \text{ Å for } j = 2, 4, 6, \ldots, 34, 36. \quad (51)$$

Figures 2, S4 show the corresponding rotating molecular wheel in the pseudo-rotating bearing of the tubular rotor La-[B_2@B_{18}]-La, for the first half cycle of the wheel ($0° \leq \varphi_j \leq 180°$, $0 \leq j \leq 18$) and the simultaneous first phase-shifted full cycles of the nuclei of the bearing. One readily notices that the pseudo-rotational sequences can be subdivided into four "radial events" (a), (b), (c), (d). For convenience, these events will be described for the pseudo-rotational sequence of the nucleus at reference angle $\Phi_1 = 10\ °$, cf. eqn. (49); the corresponding radii $R_j(\varphi_j)$ are listed in Table S2a, and they are also obvious in Figures S6a and S7a. (a) Namely for most of the time, specifically when the azimuthal angle of the wheel φ_j is between 0 ° and approximately 70 ° (j = 0 – 7, i = 18,1 – 4, cf. eqn. (47b), (47c)) and then again between about 130 ° and 180 ° (j = 13 – 18, i = 7 - 9), the nucleus at $\Phi_1 = 10°$ stays on an "inner circle" with radial values $R_j(\varphi_j) \approx 2.3$ Å. (b) Then at $\varphi_j \approx 80°$ (j = 8, i(TS) = 4) it switches rather quickly from the inner circle to the outer one, at $R_j(\varphi_j) \approx 2.6$ Å. (c) It stays on the "outer circle" for just a rather short time, specifically for $90° <\approx \varphi_j <\approx 110°$ (j = 9-11, i = 5-6). (d) Finally, at $\varphi_j \approx 120°$ (j = 12, i(TS) = 6) it switches back from the outer circle to the inner one. Equivalent events occur for all nuclei of the bearing at the other reference angles Φ_i, but they are phase-shifted with respect to the equivalent switches at Φ_{i-1}. The preference of the rather extended "inner" radial circle may be rationalized as consequence of the attractive bonds of the atoms of the wheel and several neighbor atoms which sit near to the short ellipsoidal axis of the bearing. In contrast, the rather short "outer" radial circle is due to the lack of any bonds between the atoms of the wheel and those atoms of the bearing which sit in orthogonal positions, near to the long ellipsoidal axis of the bearing.

Finally, the cyclic sequences of the nuclear cylindrical coordinates of the two metal nuclei (i=21,22) are

$R_{21}(\varphi_j) = R_{22}(\varphi_j) = 0$ Å for j =1, 2, 3, 4, ….,35, 36,

$\Phi_{21}(\varphi_j) = \Phi_{22}(\varphi_j) = 0°$ for j =1, 2, 3, 4, ….,35, 36,

(the value "0°" is arbitrary and irrelevant.)

$Z_{21}(\varphi_j) = - Z_{22}(\varphi_j) = Z_{21}^{GM} = 2.3981$ Å for j = 1, 3, 5, …, 33, 35,

$Z_{21}(\varphi_j) = - Z_{22}(\varphi_j) = Z_{21}^{TS} = 2.3916$ Å for j = 2, 4, 6, …, 34, 36. (52)

One may say that the metal nuclei are "spectators" of the rotating molecular wheel in the pseudo-rotating tubular bearing: They just stay at opposite positions of the cylindrical axis, with entirely negligible motions along the z-axis.

SI VIII: Rotational and pseudo-rotational paths of the nuclei of the oriented tubular rotor La-[B_2@B_{18}]-La

This investigation of the oriented tubular rotor La-[B_2@B_{18}]-La has started from the cyclic sequence which leads from the reference global minimum structure GM_1 *via* the transition state $TS_{1,2}$ and then *via* GM_2, $TS_{2,3}$, GM_3, …, $TS_{17,18}$, GM_{18}, to the reference transition state $TS_{18,1}$, and finally back to GM_1, cf. Subsections SI I and SI II and eqn. (47). Subsequently, Subsection SI VII has shown that this is equivalent to an alternative sequence for the mechanism of the rotating molecular wheel (B_2) in the oriented pseudo-rotating tubular bearing (B_{18}). Specifically, the wheel rotates in 36 cyclic steps, from azimuthal angle $\varphi_{j=1}$ = 10 °*via* $\varphi_2 = 20°$, $\varphi_3 = 30°$, …, $\varphi_{35} = 350$ °, $\varphi_{36} = 360° \equiv 0°$, and finally back to $\varphi_{37} \equiv \varphi_1 = 370° \equiv 10$ °, labeled by j = 1, 2, 3, …, 34, 35, 36 and 37(≡1, modulo 36), respectively. At the same time, the eighteen boron nuclei of the tubular bearing at the reference angles $\Phi_i = 10°, 30°, …., 350°$ pseudo-rotate along 36 positions on pseudo-rotational paths, with the same labels j = 1, 2, 3, …, 35, 36, and 37 ≡ 1 (modulo 36), respectively. The pseudo-rotational positions for j = 1, 2, …, 18 are the same as for j = 19, 20, …, 36, i. e. when the wheel rotates by a full cycle, then the nuclei of the bearing perform two pseudo-rotational cycles. It suffices to know the pseudo-rotational sequence of the boron nucleus at $\Phi_1 = 10$ ° - from this, the pseudo-rotational sequences of the nuclei at the other reference angles $\Phi_2 = 30°$, $\Phi_3 = 50$ °etc. can be generated by simple recipes, cf. eqns. (45), (46). At the same time, the metal nuclei stand practically still, except for extremely small amplitude vibrations in opposite directions along the z-axis.

The goal of this Sub-section SI VIII is to extend the 36 sets of rotational and pseudo-rotational positions of the nuclei of the tubular rotor La-[B_2@B_{18}]-La labeled by j=1,2, …., 36, 37≡1 by a set of 18+2+2=22 continuous paths which lead through, or close to the coordinates for the pseudo-rotational sequences of the nuclei of the bearing, through the coordinates for the rotational sequences of the nuclei of the wheel, and for the metal nuclei. This set of paths will be called the "rotational/pseudo-rotational path" of the tubular rotor. Its construction is divided into three parts, namely first for the pseudo-rotating nuclei of the bearing, second for the rotating nuclei of the wheel, and third for the metal nuclei.

For the first task, it suffices to construct the pseudo-rotational path which leads through, or close to the coordinates of the pseudo-rotational sequence of the boron nucleus of the bearing at the reference angle $\Phi_{i=1}$ = 10 °. The remaining pseudo-rotational paths for the nuclei of the bearing at the other reference angles Φ_i, i = 2, 3, …, 18 can be generated by rotations of the "first" path by i*20 °, with alternating reflections at the x-y-plane and with phase shifts, in accord with eqns. (45), (46).

To construct the pseudo-rotational path of the nucleus of the oriented tubular bearing of La-[B_2@B_{18}]-La at $\Phi_{i=1}$ = 10 °, the sequence of 36 pseudo-rotational positions with cylindrical coordinates $\{R_j(\varphi_j),\ -\Delta\Phi_j(\varphi_j),\ |Z_j(\varphi_j)|\}$, j=1,2,…,36 (discarding those for j=0 because they are equivalent to j=36) should be extended to corresponding continuous functions depending on the azimuthal angle φ of the wheel, subsect to two criteria: (a) They should be in accord with the symmetries (48) of the discrete sequences $\{R_j(\varphi_j), -\Delta\Phi_j(\varphi_j), |Z_j|(\varphi_j)\}$ which are imposed by the C_{2h} symmetries of the reference $TS_{18,1}$ and the reference GM_1. (b) For $\varphi \rightarrow \varphi_j$, the continuous functions should approach the discrete values of the coordinates, $\{R_j(\varphi_j), -\Delta\Phi_j(\varphi_j), |Z_j|(\varphi_j)\}$. A solution of this problem is suggested by Figure S7a which shows the discrete coordinates of the nucleus of the bearing at Φ_1 = 10 after back-rotation from φ_j by Φ_1 = 10° to $\phi_j = \varphi_j$ - 10 °. Accordingly, the two criteria are satisfied by (a) corresponding representations of the continuous functions by symmetry-adapted Fourier series depending on $\phi_j = \varphi_j$ - 10 °, and (b) by least squares fits of the Fourier series to the discrete coordinates at the pseudo-rotational nuclear positions labeled j = 1, 2, …, 36. Specifically, we define

$$\text{(a) } R_j(\varphi_j) = R(\varphi_j - 10°) = R(\phi_j) \tag{53a}$$

together with the symmetry adapted Fourier series

$$R_M(\phi) = \Sigma_{\mu=0}^{M} c^{(R)}_{\mu} \cos(2\,\mu\,\phi) \tag{53b}$$

of order M, with radial Fourier coefficients $c^{(R)}_{\mu}$ such that

$R_M(\phi_j) \rightarrow R_j(\varphi_j)$ for increasing values of M. (53c)

Likewise

$-\Delta\Phi_j(\varphi_j) = -\Delta\Phi(\varphi_j - 10°) = -\Delta\Phi(\phi_j)$ (54a)

together with the symmetry adapted Fourier series

$-\Delta\Phi_M(\phi) = \Sigma_{\mu=1}^{M} c^{(\Delta\Phi)}_{\mu} \sin(2\,\mu\,\phi)$ (54b)

of order M, with angular Fourier coefficients $c^{(\Delta\Phi)}_{\mu}$ such that

$-\Delta\Phi_M(\phi_j) \rightarrow -\Delta\Phi_j(\varphi_j)$ for increasing values of M, (54c)

as well as

$|Z_j|(\varphi_j) = |Z|(\varphi_j - 10°) = |Z|(\phi_j)$ (55a)

together with the symmetry adapted Fourier series

$|Z_M|(\phi) = \Sigma_{\mu=0}^{M} c^{(Z)}_{\mu} \cos(2\,\mu\,\phi)$ (55b)

of order M, with Fourier coefficients $c^{(Z)}_{\mu}$ for |Z| such that

$|Z_M|(\phi_j) \rightarrow |Z_j|(\varphi_j)$ for increasing values of M. (55c)

The Fourier coefficients in the expressions (53b), (54b), (55b) are determined by least squares fits such that

(b) $\Sigma_{j=1}^{36} [R_j(\varphi_j) - R_M(\varphi_j - 10°)]^2$ = minimum (53d)

$\Sigma_{j=1}^{36} [\Delta\Phi_j(\varphi_j) - \Delta\Phi_M(\varphi_j - 10°)]^2$ = minimum (54d)

$\Sigma_{j=1}^{36} [|Z_j|(\varphi_j) - |Z_M|(\varphi_j - 10°)]^2$ = minimum (55d)

By construction, the Fourier series (53b), (54b), (55b) satisfy the symmetry relations (48). The corresponding factor “2” in the argument of the cos- and sin-

functions accounts for two cycles along the pseudo-rotational path during a single cycle of the molecular wheel in the oriented tubular bearing.

The Fourier series (53b), (54b), (55b) serve as approximations to the ideal set of continuous functions $\{R(\varphi - 10°), -\Delta\Phi(\varphi - 10°), |Z|(\varphi - 10°)\}$, depending on the number M+1 (or M) of Fourier coefficients. In practice, the choice of M calls for a compromise: On the one hand, increasing numbers M allow the continuous functions to approach the discrete values better and better, cf. eqns. (53c), (54c), (55c). On the other hand, increasing numbers M cause artificial wiggles of the smooth functions. Systematic investigations reveal that M = 8 is a satisfactory compromise. The corresponding Fourier coefficients are

$$c^{(R)}_{\mu}\,(\text{Å}) = 2.349, -0.114, 0.134, -0.058, 0.023, -0.003, -0.016, 0.006, -0.008 \quad \text{for } \mu = 0 - 8, \tag{53e}$$

$$c^{(\Delta\Phi)}_{\mu}\,(°) = -1.568, 0.306, -0.048, -0.424, -0.203, -0.066, 0.000, 0.008 \quad \text{for } \mu = 1 - 8, \tag{54e}$$

$$c^{(Z)}_{\mu}\,(\text{Å}) = 0.788, 0.056, 0.005, 0.028, -0.023, 0.016, 0.001, -0.002, 0.003 \quad \text{for } \mu = 0 - 8. \tag{55e}$$

These Fourier coefficients are robust with respect to their numbers M+1 (or M).

The resulting functions $\{R_{M=8}(\varphi - 10°), -\Delta\Phi_{M=8}(\varphi - 10°), |Z|_{M=8}(\varphi - 10°)\}$ are documented in Figure S6 and S7a. They establish the pseudo-rotational path of the nucleus of the bearing at the reference angle $\Phi_{i=1} = 10°$, back-rotated by - 10 °. The corresponding paths of the nuclei of the bearing centered at Φ_i, i = 2, 3, …, 18 are generated by forward rotation by 10 °for i=1, and then by sequential steps of $\Delta\Phi = 20°$, with alternating reflections at the x-y-plane, in accord with the previous recipe SI VII(f), cf. eqn. (46). The result is shown in Figures 2 and S4a.

The second and third tasks of this Subsection are rather easy, compared to the first one. Namely the rotational paths of the two nuclei (n=19,20) of the molecular wheel are nearly circular. The explicit expressions are

$$R_{19}(\varphi) = R_{20}(\varphi) = R_w + \Delta R_w \cos(18\varphi),$$
$$R_w = .5(R_{19}^{GM} + R_{19}^{TS}) = 0.81795 \text{ Å},$$
$$\Delta R_w = .5(R_{19}^{TS} - R_{19}^{GM}) = 0.00025 \text{ Å},$$

$$\Phi_{19}(\varphi) = \varphi, \quad \Phi_{20}(\varphi) = \varphi + 180°,$$

$$Z_{19}(\varphi) = - Z_{20}(\varphi) = Z_{19}^{GM} \sin(9\varphi),\ Z_{19}^{GM} = -0.0177 \text{ Å}, \quad (56)$$

cf. eqn. (51). The associated paths of the metal nuclei are along the Z-axis,

$$R_{21}(\varphi) = R_{22}(\varphi) = 0 \text{ Å},$$

$$\Phi_{21}(\varphi) = \Phi_{22}(\varphi) = 0°,$$

$$Z_{21}(\varphi) = -Z_{22}(\varphi) = Z_m + \Delta Z_m \cos(18\varphi),$$
$$Z_m = .5(Z_{21}^{GM} + Z_{21}^{TS}) = 2.39485 \text{ Å},$$
$$\Delta Z_m = .5(Z_{21}^{TS} - Z_{21}^{GM}) = -0.00325 \text{ Å}, \quad (57)$$

cf. eqn. (52), i. e. the two metal nuclei serve as spectators which are practically fixed at the cylindrical axis, except for tiny modulations.

SI IX: Support of the model of the rotating molecular wheel in the pseudo-rotating bearing by vector arrow plots of two selected normal modes of La-[B_2@B_{18}]-La

Subsection SI VII reveals the oriented model La-[B_2@B_{18}]-La as tubular rotor with molecular wheel (B_2) rotating in the pseudo-rotating tubular bearing (B_{18}). To support this picture, we shall now add information about the directions of the nuclear motions which lead along these sequences. For this purpose, we shall first consider the nuclear motions which are directed from the reference transition state $TS_{18,1}$ to the neighboring reference global minimum structure GM_1. The results will be extrapolated to the nuclear motions from the other $TS_{k,k+1}$ to the neighboring GM_{k+1}. By analogy, we shall also consider the nuclear motions which are directed (approximately) from GM_1 to the next neighboring $TS_{1,2}$. This will be extrapolated to the nuclear motions from the other GM_k to the next neighboring $TS_{k,k+1}$. The presentation and analyses below are rather detailed for the nuclear motions from the TSs to the GMs and more compact for the analogous motions from the GMs to the TSs. Finally, we shall arrive at a set of nuclear motions which are directed along the pseudo-rotational sequence (47).

In general, the nuclear motions which lead across a transition state toward the next global minimum structure are specified by the transition state's normal mode with imaginary frequency. In the present reference case of $TS_{18,1}$, these motions are illustrated by the vector arrow plot of the normal mode with imaginary frequency ($|\hbar\omega_i^{TS}|$ = 217.90 h c cm^{-1}, IRREP b_g), cf. Figure S3b. The

vectors at nucleus i of the reference $TS_{18,1}$ will be denoted by Cartesian coordinates, $\mathbf{\Delta Q_i^{TS}} = (\Delta X_i^{TS}, \Delta Y_i^{TS}, \Delta Z_i^{TS})$. They are plotted with finite lengths and arbitrary scaling, and with their tails attached to the positions of nucleus i, as specified in Subsection SI II and in Table S2a. The finite vectors $\mathbf{\Delta Q_i^{TS}}$ are proportional to infinitesimally small vectors, $\mathbf{\Delta Q_i^{TS}} \sim \mathbf{dQ_i^{TS}}$, which cannot be illustrated. The advantage of using finite vectors $\mathbf{\Delta Q_i^{TS}}$ for illustrations is that they show the directions of the $\mathbf{dQ_i^{TS}}$, and they also illustrate the relative lengths of the $\mathbf{dQ_i^{TS}}$ for the different nuclei. In a classical picture, the $\mathbf{dQ_i^{TS}}$ are proportional to the nuclear velocities $\mathbf{dQ_i^{TS}}/dt$. With proper scaling of the time interval Δt, one may set $\mathbf{dQ_i^{TS}}/dt = \mathbf{\Delta Q_i^{TS}}/\Delta t$. That means that the classical nuclear velocities are along the directions of the vectors $\mathbf{\Delta Q_i^{TS}}$, and "long" and "short" vectors $\mathbf{\Delta Q_i^{TS}}$ correspond to "fast" and "slow" classical velocities. One may define a semiclassical normalization of the vectors and the related time interval Δt, (somewhat arbitrarily, of course) by setting the related classical nuclear kinetic energies equal to the quantum energy of the local b_g mode with imaginary frequency, $.5(|\hbar\omega_i^{TS}| = .5\ \Sigma_i,\ m_i,\ (\mathbf{dQ_i},^{TS}/dt)^2 = .5\ \Sigma_i,\ m_i,\ (\mathbf{\Delta Q_i},^{TS}/\Delta t)^2$.

Close inspection of the vector arrows $\mathbf{\Delta Q_i^{TS}}$ of the b_g mode with imaginary frequency for the reference $TS_{18,1}$ in Figure S3b reveals that there are just four prominent nuclei of the bearing which move rather rapidly, all with the same speed, namely the quadruplet of nuclei labeled i(TS) = 4, 6, 13, 15; according to eqn. (47) (cf. Table S2a and Figure 7a), these correlate with labels j = 8, 12, 26, 30, respectively. Their directions are in accord with IRREP b_g; in particular, the vector arrows for nucleus 4 and the opposite nucleus 13 point toward decreasing radii, whereas the vector arrows for nucleus 6 and the opposite nucleus 15 point to increasing radii. In contrast, all other nuclei of the bearing move rather slowly. At the end of this Subsection, this curious result will provide a nice confirmation of the scenario of the rotating wheel in the pseudo-rotating tubular bearing. As first hint to this end, we notice that the two labels i(TS) = 15 and 13 of the nuclei which move rapidly towards larger and smaller radii, correlate with the second "radial event" (b) at $\varphi_{j=8} = \varphi_{k,k+1=4,5}$ (j=8, k(TS)=4) and with the forth one (d) at $\varphi_{j=12} = \varphi_{k,k+1=6,7}$ (j=12, k(TS)=6) which have been diagnosed towards the end of the Sub-section SI VII, namely (b) the rapid transitions from the "inner radial circle" to the "outer" one, (d) and back, during the first pseudo-rotational sequence i.e. during the first half cycle of the wheel. Specifically, when the wheel moves from $\varphi_{k,k+1=18,1} = 0\,°$ *via* $\varphi_{1,2}$, $\varphi_{2,3}$, $\varphi_{3,4}$ to $\varphi_{4,5}$ and then *via* $\varphi_{5,6}$ to $\varphi_{6,7}$, then the labels of the nuclei of the bearing which sit at the reference site at $\Phi_{i=1} = 10\,°$ vary from the initial i=1 *via* 18, 17, 16 to 15 (*sic!*) and then *via* 14 to 13 (*sic!*), respectively. Thus as long as the wheel moves from $\varphi = \varphi_{k,k+1=18,1} = 0°$ to $\varphi_{3,4} = 70\,°$, the radius of nucleus i=1 of the bearing at $\Phi_{i=1} = 10\,°$ remains at the "inner circle, $R_k^{TS} \approx 2.3$ Å, corresponding to the "radial event (a)". When the wheel

arrives at $\varphi_{4,5} = 80°$ and subsequently at $\varphi_{6,7} = 120°$, then the nucleus at $\Phi_{i=1} = 10°$ moves rapidly from the "inner radial circle" to the "outer" one ($R_{k=5}^{TS} \approx 2.6$Å) (event (b)), and back (event (d)), respectively. The opposite nuclei 6 and 4 take the same roles during the second pseudo-rotational sequence i. e. during the second half cycle of the wheel.

As expected for the motion from $TS_{18,1}$ ($\varphi_{j=1} = \varphi_{k,k+1=18,1} = 0$ ◦) to GM_1 ($\varphi_{j=2} = \varphi_{k=1} = 10$ ◦), the vector arrows at the two nuclei of the wheel (i=19,20) point to (anti-clockwise) rotation of the wheel with respect to the bearing. These vectors at the wheel are shorter than the prominent ones at the nuclei of the bearing (i(TS) = 4, 6, 13, 15), i. e. the pseudo-rotational speed of the boron nuclei during the transitions from short to long radii, and back (events (b) and (d)) is even higher than the speed of the rotating nuclei of the wheel. For comparison, the metal nuclei stand practically still - this confirms their role as "spectators" sitting on the cylindrical axis of the tubular rotor La-[B_2@B_{18}]-La.

Starting from the nuclear motions which lead from the reference $TS_{18,1}$ to the reference GM_1, as illustrated in Figure S3b, it is straightforward to generate the corresponding vector arrow plots of the nuclear motions which point from arbitrary $TS_{k,k+1}$ to the next GM_{k+1}, namely by k-fold applications g^k , $\tilde{g}^k$ or $g^{\approx k}$ of one of the three equivalent generators g, $\tilde{g}$ or $g^{\approx}$ which have been introduced in Sub-sections SI I and SI VII. For convenience, we shall employ $\tilde{g}^k$ for the generation, and $g^{\approx k}$ for the analysis. From a mathematical perspective, we recall that the set of operators $\{\tilde{\boldsymbol{e}}^{\sim}, \tilde{g}, \tilde{g}^2, \ldots, \tilde{g}^{17}\}$ establishes the cyclic group $\tilde{C}_{18}(M)$ which can be applied to any molecular structure, cf. Sub-section SI I. It can be applied, therefore, not only to the original $TS_{18,1}$, as done above, but also to a modified version of $TS_{18,1}$ with the nuclear positions shifted by infinitesimal or by finite displacements $\mathbf{dQ_n^{TS}}$ and $\mathbf{\Delta Q_n^{TS}}$. That means it can be applied to the tails and to the heads of the vector arrows, with the tails fixed at the nuclear positions of $TS_{18,1}$, or in other words it can be applied to the set of vector arrows which are shown in Figure S3b.

Applications of $\tilde{g}, \tilde{g}^2, \ldots, \tilde{g}^8$ to the vector arrows shown in Figure S3b for the b_g mode with imaginary frequency of the reference $TS_{18,1}$ generate the vector arrow plots of the corresponding b_g modes of $TS_{1,2}$, $TS_{2,3}$, …., $TS_{8,9}$. The superposition of these vector arrow plots is shown in Figure S3c. Accordingly, these transition states are crossed sequentially during the first half cycle of the wheel, and at the same time during the first full pseudo-rotational cycle of the bearing. Indeed, the vector arrows attached to the two nuclei of the wheel support the picture of the half-cycle rotation of the wheel. Likewise, the arrows attached to the eighteen nuclei of the bearing support the picture of a full cycle of pseudo-rotation, with

the corresponding four "radial events" (a)-(d). In contrast, the metal nuclei stand practically still as spectators on the nuclear axis. Equivalent results are obtained for the second half rotational cycle of the wheel and for the simultaneous second full pseudo-rotational cycle of the bearing. In any case, by construction all the corresponding nuclear motions are directed from the TSs to the next GMs beyond the reference GM_1, specifically to GM_2, GM_3, …, GM_9.

For the analysis of the results shown in Figure S3c it is convenient to switch from the generator $\tilde{g}$ to $\tilde{g}^{\approx}$ and to consider a magnification of the corresponding pseudo-rotational sequence of the vectors which are attached to the positions of the nucleus of the bearing at the reference angle $\Phi_{i=1} = 10°$. The magnification is illustrated in Figure S7b where it is back-rotated by $-\Phi_{n=1} = -10°$ such that it appears as centered at 0 ° - this back-rotation allows an illuminating comparison with the pseudo-rotational sequence of positions shown in Figure S7a. Apparently, the arrows attached to the nuclear positions for the transition states point toward the positions of the next neighbouring global minimum structures. Obviously, the arrow plots shown in Figures S3c and S7b support the picture of the rotating wheel in the pseudo-rotating bearing.

Next we seek for the analogous vector arrow plot of a normal mode of the reference global minimum structure GM_1 with the nuclear motions directed from GM_1 to the next neighboring $TS_{1,2}$. There is, however, no rigorous rule for the choice of the suitable mode of GM_1; in fact, it is not even guaranteed that such normal mode exists – hence we should anticipate that whatever choice we make, the nuclear arrows may not point directly to the next $TS_{1,2}$, but just approximately. In practice, we apply three criteria for the proper choice of the normal mode of GM_1 which should point (approximately) to $TS_{1,2}$. The first criterion is a rigorous one i. e. the normal mode must have IRREP b_g of the local C_{2h} symmetry of GM_1, because this is the only IRREP which allows the vector arrows for the two nuclei of the molecular wheel to be directed toward rotation. The second criterion is empirical, i. e. we request that the vibrational frequency of the b_g mode of GM_1 should be close to the absolute value of the imaginary frequency mode of the reference $TS_{18,1}$ ($|\hbar\omega_i^{GM}|$ = 217.90 h c cm^{-1}). This criterion ensures that the resulting model potential V(φ) for the rotating wheel in the pseudo-rotating bearing is approximately cosinusoidal, cf. Figure 3 and S5; alternative choices with extremely low or high b_g mode frequencies at GM_1 compared to $TS_{18,1}$ would imply model potentials with sharp peaks at the potential minima or at the potential barriers – this would appear as unrealistic. Figure S3a shows that this second criterion suggests the b_g mode labeled ν^{GM} =8 ($\hbar\omega_8^{GM}$ = 234.79 h c cm^{-1}). The third criterion is again empirical, i. e. we request that the chosen b_g mode of GM_1 must not direct the nuclear motions entirely away from $TS_{1,2}$. For this

criterion, we have also checked the two b_g modes of GM_1 with the next higher or the next lower frequencies, compared to $v^{GM} = 8$. It turns out that the next higher frequency b_g mode labeled $v^{GM} = 13$ ($\hbar\omega_{13}^{GM} = 342.89$ h c cm^{-1}) kicks the two metal nuclei away from the cylindrical axis – this is inacceptable. The next lower frequency b_g mode labeled $v^{GM} = 2$ ($\hbar\omega_{2}^{GM} = 156.58$ h c cm^{-1}) points away from $TS_{1,2}$ – this is again inacceptable. For our purpose we choose, therefore, the b_g mode labeled $v^{GM} = 8$ ($\hbar\omega_{8}^{GM} = 234.79$ h c cm^{-1}). Its vector arrow plot is shown in Figure S3b.

After the detailed discussion of the vector arrow plot of the b_g mode of the reference $TS_{18,1}$ shown in Figure S3b, one immediately recognizes that the chosen b_g mode of the reference GM_1 displays a similar pattern. Accordingly, the vector arrows at the nuclei of the wheel (i=19,20) point to (anti-clockwise) rotation of the wheel, and there are just four prominent nuclei of the bearing which move rather quickly, namely those labeled i(GM) = 4, 7, 13, 16. According to eqn. (47), these labels correlate with j = 7, 13, 25, 31, respectively. All other boron nuclei move rather slowly, and the metal "spectators" stand practically still. For more quantitative comparison, let us recall that the chosen b_g mode of the reference $TS_{18,1}$ has analogous four nuclei of the bearing which promote rapid pseudo-rotation, namely those labeled i(TS) = 4, 6, 13, 15, correlating with j = 8, 12, 26, 30, cf. eqn. (47). Obviously, the quadruplets of labels j for the chosen b_g modes of GM_1 and $TS_{18,1}$ are next neighbors to each other. This implies that the mechanism of the pseudo-rotation with four "radial events" – (a) rather long circulation at small radii $R_j \approx 2.3$ Å, (b) rapid transition from small to large radii, (c) short circulation at large radii $R_j \approx 2.6$ Å, (d) back-transition to small radii $R_j \approx 2.3$ Å, - which has been diagnosed in Subsection SI VII, is confirmed not only by the nuclear motions of $TS_{18,1}$ and the $TS_{k,k+1}$ which are generated from $TS_{18,1}$, but also by those of GM_1 and the GM_k which are generated from GM_1. In contrast with the prominent four arrows for the pseudo-rotation of the bearing of $TS_{18,1}$ which are larger than the two arrows for the rotation of the wheel, the prominent four arrows for the pseudo-rotation of the bearing of GM_1 are, however, smaller than those for the rotation of the wheel. This suggests that the events (b) and (d) occur with highest speed when the molecular wheel has moved from $\varphi_{j=1} = 0$ for $TS_{18,1}$ to azimuthal angles $\varphi_j = 80°, 120°, 260°, 300°$ for transitions states, (j = 8, 12, 26, 30), whereas the neighboring angles 70 °, 130 °, 250 °, 310 ° for global minimum structures (j = 7, 13, 25, 31) mark the related on- or off-sets of the events (b) and (d).

Starting from the chosen b_g mode of the reference GM_1 (Figure S3b), one can generate and analyze the b_g modes of the sequence of the other GM_2, GM_3, …, GM_{18} in the same way as shown above for the transition states, i. e. by

applications of $\tilde{g}$, $\tilde{g}^2$, …, $\tilde{g}^{17}$ for generation and $g^{\approx}$, $g^{\approx 2}$, …, $g^{\approx 17}$ for analysis. The resulting superposition of the first nine vector arrow plots for the b_g modes of GM_1 – GM_9 is documented in Figure S3c, together with the vector arrow plots for the neighbouring transition states. A magnification of the vector arrow plot in the domain of the nucleus at the reference angle $\Phi_1 = 10\,°$ is shown in Figure S7b, together with the vector arrows for the neighbouring transition states.

Figure S3c shows the superposition of all vector arrow plots of the chosen b_g normal modes for the transition states and for the global minimum structures. Magnifications are shown in Figure S7b. These Figures confirm the nuclear motions of the tubular rotor La-[B_2@B_{18}]-La with its molecular wheel (B_2) rotating in the pseudo-rotating tubular bearing (B_{18}).

References

33. C. Adamo and V. Barone, *J. Chem. Phys.*, 1999, **110**, 6158.
34. R. Krishnan, J. S. Binkley, R. Seeger and J. A. Pople, *J. Chem. Phys.*, 1980, **72**, 650.
35. D. Feller, *J. Comput. Chem.*, 1996, **17**, 1571.
36. L. Schuchardt, B. T. Didier, T. Elsethagen, L. Sun, V. Gurumoorthi, J. Chase, J. Li and T. L. Windus, *J. Chem. Inf. Model.*, 2007, **47**, 1045.
37. M. J. Frisch, *et al.*, *Gaussian 09, Revision D.01*, Gaussian Inc., Wallingford, CT, 2009.